Received: 22 February 2019 | Revised: 1 December 2019 | Accepted: 18 December 2019

DOI: 10.1002/ldr.3530

RESEARCH ARTICLE

WILEY

A new analysis approach for long-term variations of forest loss, fragmentation, and degradation resulting from road-network expansion using Landsat time-series and object-based image analysis

Zeinab Shirvani | Omid Abdi | Manfred F. Buchroithner

Department of Geosciences, Institute for Cartography, Faculty of Environmental Sciences, TU Dresden, Dresden, Germany

Correspondence
Zeinab Shirvani, Department of Geosciences, Institute for Cartography, Faculty of Environmental Sciences, TU Dresden, 01069 Dresden, Germany.
Email: zeinab.shirvani@gmail.com; zeinab.shirvani@tu-dresden.de

Abstract

Despite facilitating transport by low-volume roads for multiple purposes, these roads also open corridors to the remote pristine forests and accelerate forest dynamics with deleterious consequences to the forest functionalities and indigenous inhabitants. We assessed the spatial variations of Hyrcanian forest loss, fragmentation, and degradation resulting from the expansion of rural, logging, and mine roads between 1966 and 2016 in northeast Iran. Various data were employed to generate a precise road network; the density of road segments was weighted on the basis of their carrying capacity during 1966–1986, 1986–2000, and 2000–2016. Three dimensions of forest changes were retrieved using the Landsat time-series and object-based image analysis. The spatial patterns of high rates of forest changes were clustered using spatial autocorrelation indicators. The spatial regression models were carried out to explore relationships between forest change and road expansion. The results showed that rural roads were upgraded but forest and mine roads remarkably expanded in recent decades. The spatial variations of forest-dynamic patterns have been changing from forest loss (1966–2000) to forest fragmentation and degradation (1986–2016). The high density of rural roads was significant on the high rates of forest loss and fragmentation during 1966–2000, and the expansion of forest and mine roads significantly intensified the rates of fragmentation and degradation during 1986–2016. Our findings suggest for mitigating destructive schemes over Hyrcanian forests, developing either protected areas or joining unprotected forests to the reserved areas should be prioritized.

KEYWORDS

forest changes, low-volume roads, OBIA, spatial indicators, spatial models, time series

1 | INTRODUCTION

Although low-volume roads facilitate transport to rural communities, timber harvesting, mining operations, and resource management (Douglas, 2017), paradoxically, accelerate deforestation, forest fragmentation, and degradation (Chomitz & Gray, 1996; Trombulak & Frissell, 2000) with deleterious impacts on flora and fauna communities such as physical disturbances of forests, chemical and nutrient contaminations,

heavy local mortality of species, proliferation of invasive species, and facilitation of anthropogenic invasions in the forest ecosystem (Kleinschroth, Gourlet-Fleury, Gond, Sist, & Healey, 2016; Laurance, Goosem, & Laurance, 2009; Trombulak & Frissell, 2000). Although the impacts of the expansion of large-scale road networks on forest fragmentation are well documented for different forest ecosystems (Alamgir et al., 2017), the holistic effects of expanding low-volume road networks on intensifying deforestation, forest fragmentation, and degradation are less explored, especially in sensitive ecosystems like Hyrcanian forests with high species diversity and environmental values.

Forest loss, fragmentation, and degradation are distinctly different processes. Forest loss results from the conversion of forests to non-forest lands by direct anthropogenic activities such as clear-cutting of forests to establish farmlands or settlements (Shirvani, Abdi, Buchroithner, & Pradhan, 2017; Tejaswi, 2007); forest fragmentation refers to the breaking up of continuous forest areas into smaller patches resulting from natural processes or deforestation (Laurance, 2000; Tejaswi, 2007); and forest degradation is a consequence of declining biomass within forests due to intensive human-natural disturbances such as logging, mining, droughts, forest fires, and floods (Tejaswi, 2007).

Rural roads profoundly increase spatial patterns of forest loss because new roads raise the accessibility to the remote forests and have a pivotal role in increasing population in the frontiers of forests and lead to forest colonization by clear-cutting to establish farmlands and settlements (Shirvani et al., 2017) or smuggling timbers (Ali, Benjaminsen, Hammad, & Dick, 2005). Laurance et al. (2002) confirmed the significant impacts of a high density of paved roads and rural population on the high rates of forest loss in Brazilian Amazonia. Barber, Cochrane, Souza, and Laurance (2014) concluded that roughly 95% of all Amazonian deforestation located within a distance of 5.5 km from the road network, and the unprotected areas nearby roads have received a remarkable deforestation compared with the protected areas. In remote forests, the effects of paved and unpaved roads on forest loss might be higher than the developed areas due to the lack of conservation programs (Jusys, 2016). Even a small increase in road density can cause extensive deforestation (Mena, Laso, Martinez, & Sampedro, 2017). Moreover, expanding and upgrading low-volume roads open up corridors between settlement areas and remote pristine forests for logging and mining operations that may lead to extensive deforestation and forest degradation, especially in developing countries (Ali et al., 2005; Laurance et al., 2001). However, forest roads have an irrefutable role in logging (Sessions, 2007) and fire-suppressing operations (Abdi et al., 2018; Narayanaraj & Wimberly, 2012). The proliferation of logging roads is considered as a major driver of forest fragmentation and degradation (Arima, Walker, Perz, & Caldas, 2005). They adversely affect the biodiversity and forest functionalities such as a major alteration in the forest habitat, soil erosion (Douglas, 2003; MacDonagh et al., 2010; Malmer & Grip, 1990), hydrological effects (Boston, 2016; Bruijnzeel, 2004; La Marche & Lettenmaier, 2001; Sidle, Sasaki, Otsuki, Noguchi, & Rahim Nik, 2004; Trombulak & Frissell, 2000), and disrupting wildlife populations, their movement, and behavior (Lees & Peres, 2009; Van Der Hoeven et al., 2010; Clements et al., 2014; Boston, 2016). Likewise, widespread mining activities have remarkably increased forest loss in various forest ecosystems (Butsic, Baumann, Shortland, Walker, & Kuemmerle, 2015; Caballero Espejo et al., 2018). Mineral extraction has a strong relationship with infrastructure expansion that leads to mass migration and farming expansion into the forest frontiers results in a massive forest loss and forest degradation (Bebbington et al., 2018). In the Peruvian region of Amazonia, for example, gold mining and road construction significantly increased during 1999–2012, as only in 2008, they tripled the annual average of forest loss (Asner, Llactayo, Tupayachi, & Luna, 2013). Sonter et al. (2017) reported that mining-induced forest loss has extended to approximately 70 km from the mine frontiers, and about 9% of all Amazonian forest loss were results from mining operations, only during 2005–2015. Although many of these studies focused on the distance to roads as a main driver of deforestation and forest degradation, the impact of road types is less well documented. We argue that every road highly affects forest loss, fragmentation, and degradation within its optimal coverage area (OCA). Therefore, we will explored the weighted density of roads, which can be retrieved from the total amount of population, logging volume, and mining weight as the carrying capacity of rural, forest, and mining roads during a specific period.

The products of high-level United States Geological Survey (USGS) Landsat Surface Reflectance Climate Data Records (USGS 2018) have remarkably improved the long-term monitoring of forest dynamics (Hermosilla, Wulder, White, Coops, & Hobart, 2015; Young et al., 2017) and appraised the driving forces of forest disturbances such as anthropogenic processes, climate changes, and socioeconomic pressures at local, regional, and global levels (Kennedy et al., 2014). Hence, different approaches have been developed to visualize spatial patterns of forest loss, fragmentation, and degradation using time-series imagery from pixel to object levels (Riitters, Wickham, Neill, Jones, & Smith, 2000; Heilman, Strittholt, Slosser, & Dellasala, 2002; Desclée, Bogaert, & Defourny, 2006; Fischer & Lindenmayer, 2007; after McIntyre & Hobbs, 1999; Ernst et al., 2010; Raši et al., 2013; Newman, McLaren, & Wilson, 2014; Hermosilla et al., 2015; Uddin et al., 2015). However, some new research has demonstrated the potential of spatial autocorrelation indicators in visualizing spatial patterns of forest changes. The spatial autocorrelation approaches are robust in conceptualizing spatial relationships among features that rely on the null hypotheses in analyzing spatial patterns among the features. They statistically determine significant hot clusters, cold clusters, and spatial outliers using local spatial autocorrelation indices, *p* values, and *z* score (Anselin, Syabri, & Kho, 2006). Shirvani et al. (2017), for example, reported the good performance of local spatial autocorrelation statistics including local univariate spatial autocorrelation (LISA) for visualizing the spatial patterns of deforestation. They also used the bivariate local spatial autocorrelation (BiLISA) for visualizing the spatial patterns of deforestation induced by residential growth in the Hyrcanian region from 1972 to 2010. Although some studies proposed spatial autocorrelation indices as an appropriate alternative for landscape metrics (Fan & Myint, 2014), these indicators provide valuable attributes of fragmented patches for visualizing spatial patterns of fragmentation at class and landscape levels.

Southworth, Munroe, and Nagendra (2004) confirmed the potential of LISA for the visualization of fragmentation intensity in land-cover classes retrieved from normalized difference vegetation index. Because the local autocorrelation indicators explore the spatial relationship between a location and its neighborhoods using different connectivity approaches; therefore, the integration of traditional metrics and spatial autocorrelation indicators can be considered as a novel approach in visualizing the spatiotemporal patterns of different dimensions of forest dynamics. We argue that not only the spatiotemporal variations of loss, degradation, and fragmentation of forest areas are significant but also the spatial interdependency between the dimensions of forest changes and the expansion of low-volume roads is significant.

The growth rate of population and the demands of rural communities have caused an unprecedented competition among planners for expanding timber harvesting and mining schemes in the Hyrcanian region for several decades. Therefore, road networks are noticeably developing with weak designation as well as massive environmental and socioeconomic problems (Caspian Hyrcanian Forest Project, 2013). Hence, long-term investigation of transport development schemes along with population growth may reveal spatiotemporal negative impacts of expanding diverse road networks onto the magnitude of different types of forest changes (Caspian Hyrcanian Forest Project, 2013). This is important for the conservation, particularly to avoid the expansion of new roads in pristine forests or the remediation of available roads in favor of the forest ecosystem.

In this study, we quantify forest loss, fragmentation, and degradation resulting from expanding rural roads, forest roads, and mining roads in the Iranian Hyrcanian region for the last 50 years during three periods (1966–1986, 1986–2000, and 2000–2016). The three dimensions of forest dynamics are assessed by means of the interpretation of Landsat time series and object-based image analysis (OBIA) as well as spatial autocorrelation indicators. We test rigorous spatial dependence models to determine the relationship between the dimensions of the three forest dynamics and three road types (i.e., rural, forest, and mining roads) in the aforementioned times. Our spatial analysis is a combination of novel approaches for calculating road density and using objects for visualizing forest loss and fragmentation and analyzing Landsat time series for estimating forest degradation in the Hyrcanian region.

2 | MATERIALS AND METHODS

2.1 | Study area and data

We selected the eastern part of Hyrcanian forests in the Golestan Province, Iran, with an area of 445,000 ha (Figure 1), which were less

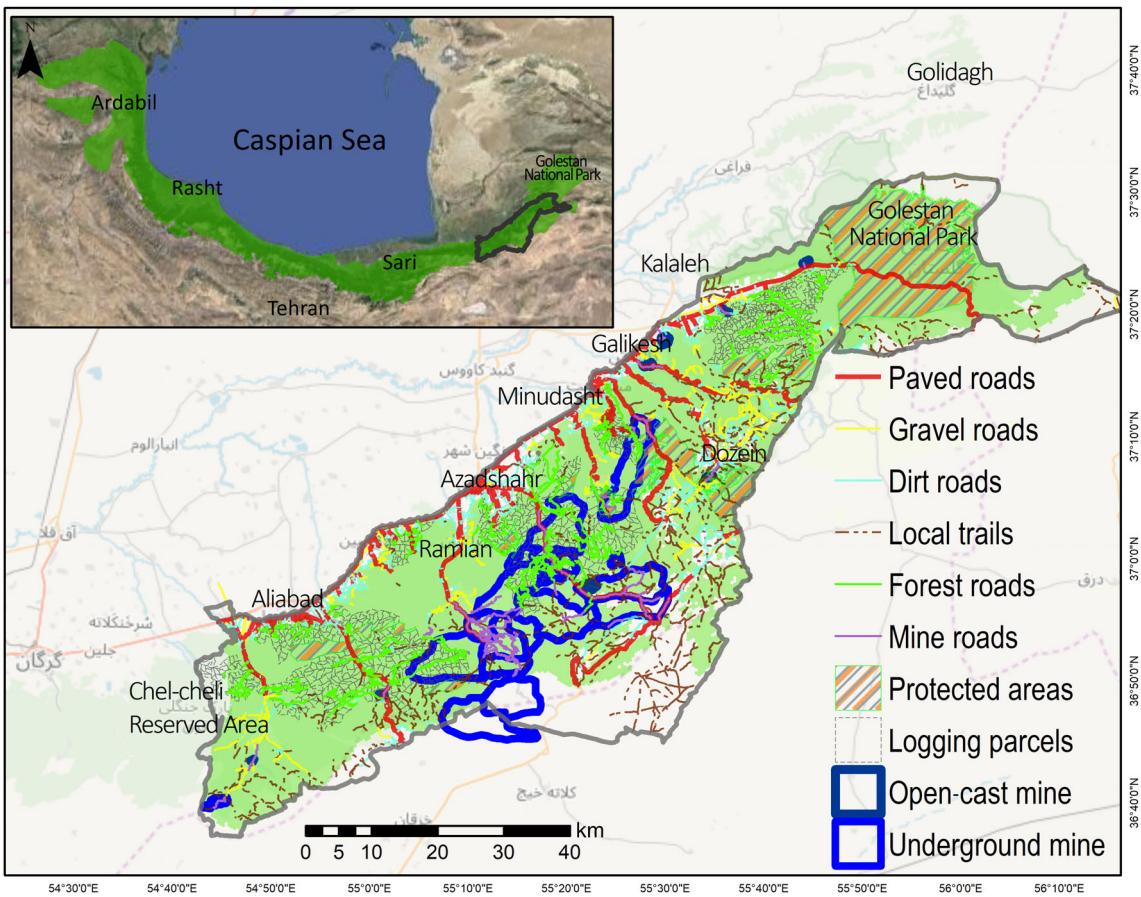

FIGURE 1 The location of study area in the Hyrcanian forests and the spatial distribution of the current forest management plans, mining plans, protected forests, and road networks in northeastern Iran [Colour figure can be viewed at wileyonlinelibrary.com]

affected by human activities in 1966 for the current research. The study area is divided into 15 rural districts including 195 villages and eight cities in 2016. The Hyrcanian deciduous broadleaved forests are the only relics of pristine temperate forests by a rich diversity of woody species (Knapp, 2005). The largest national park of Iran, Golestan National Park, is located in this region with about 50% of total mammal species and 30% of the total birds of Iran and more than 1,400 registered plant species by United Nations Educational, Scientific, and Cultural Organization in 1976 (Akhani & Ziegler, 2002; Sagheb-Talebi, Sajedi, & Pourhashemi, 2014). The majority of these forests are located in the mid-altitude (800–1,600 m) that is dominated by tree species of *Quercus castaneafolia*, *Carpinus betulus*, *Acer velutinum*, *Parrotia persica*, and *Ulmus glabra* (Sagheb-Talebi et al., 2014). Timber harvesting has begun in these forests since 1960s, as the number of Forest Management Plans (FMPs) has reached 17 cases in 2016 (Figure 1). Although the single-tree selection method is the current timber harvesting system in the FMPs, few other harvesting systems such as clear-cutting and partial cutting (e.g., unique block and shelterwood) were undertaking during the beginning time periods of logging operations in Hyrcanian forests (Badraghi, Erler, & Hosseini, 2015; Jourgholami & Majnounian, 2011). Moreover, the number of mine plans has reached 29 cases in 2016, dominantly coal and quarry mine types (Figure 1).

We collected required data from a variety of references including the aerial photos (1:20,000) of 1966; analogue topographic maps (1:50,000) of 1957; two- and three-dimensional digital topographic maps (1:25,000) of 1991 and 2003; the open-access Level 1 terrain-corrected of Landsat 1–5 multispectral scanner data obtained from 1972 to 1986 with a total of 56 candidate images; Landsat surface reflectance Level 2 science products of Landsat 4–5 Thematic Mapper, Landsat 7 Enhanced Thematic Mapper Plus, and Landsat 8 Operational Land Imager from 1986 to 2016 with a total of 278 candidate images. Population data were obtained from the National Census of Population and Housing Data (http://www.amar.org.ir) in 1966, 1986, 2001, and 2016 (Statistical Center of Iran, 1966; 1986; 1996; 2000; 2011; 2016). The data of logging volumes were extracted from the booklets of the FMPs for the parcels in the three study periods. We retrieved the time-series data of mining plans from the reports of Statistical Centre of Iran (http://www.amar.org.ir) and online database of Iranian Mining Organization (http://www.ime.org.ir) as well.

2.2 | Methods

2.2.1 | Expansion of rural, forest, and mine roads (low-volume roads)

Extraction of road networks

A combination of data from aerial photos, topographic maps, Landsat data, the maps of FMPs and mine plans, as well as Google Earth images were used to generate an accurate road network including rural, forest, and mine haul roads. We vectorized the roads of 1966 from 1:20,000 scale aerial photos and 1:50,000 scale topographic maps. The roads of 1986 and 2000 were updated using 1:25,000 digital topographic maps, the maps of the FMPs, and Landsat images. Google Earth images were used to update the changes of roads in 2016 as well. We classified the road networks into six categories on the basis of the legends of topographic maps, the layers of the FMPs, and mine plans in the studied years. Rural roads are classified as low-traffic volume roads to provide access for multiple uses in nonurban areas, recreational sites, farmlands, and rangelands (Douglas, 2017). Paved roads, gravel roads, dirt roads, and local trails are classified as rural roads. Forest roads are designed to serve logging operations, recreational and scenic attractions, and studying operations of forest ecosystems. Skid trails, as temporary pathways, are used for skidding logs to the log landings (Keller & Sherar, 2003). Mine haul roads are used for transporting variety of trucks for carrying ore and waste from different types of mines (Tannant & Regensburg, 2001).

Road density

The primary density of rural, forest, and mine roads (RD(r, f, m)) were calculated by dividing the total length of roads (L) by the extent of residential areas, logging plans, and mining plans for the three periods. The OCA of roads was determined depending on the average length of roads (RA) as Equation (1).

$$\mathrm{RD}(r,f,m)=\frac{\sum L\,(\mathrm{m})}{\mathrm{area}\,(\mathrm{ha})},\mathrm{RA}(r,f,m)=\frac{10000}{2\mathrm{RD}};\mathrm{OCA}\,(r,f,m)=\pi\times\mathrm{RA}^2. \quad (1)$$

To determine the density of roads, we weighted the road segments on the basis of their carrying capacity including population, logging volume, and material weight. Weighted road density was calculated in the neighborhoods of each hexagonal cell, as the length of the segment(s) of each road falling within the OCA multiplied by its weight (Equation 2). These weighted values refer to the rural population that has access to a rural road within a period; the total volume of logging that carried out by a forest road during the period; and the total weight of mining materials that carried out by a mine haul road during the period. The total value was divided by the OCA of the road types (Equation 2).

$$\mathrm{WRD}_j(r,f,m)=\frac{\sum_{i=1}^{n}L_{ij}\times\mathcal{W}_{ij}}{(\mathrm{OCA})}, \quad (2)$$

where WRD_j is the weighted road density of rural (r), forest (f), and mine (m) roads at the jth cell in each period; L_{ij} and $\mathcal{W}_{ij}$ represent the length and weight of segment i at the jth cell, respectively.

Changes in road density

We designed a hexagonal cell about the same size as the OCA of the roads, thus allowing us to localize the changes of road density and forest degradation within each hexagonal cell during the three time periods. The expansion of road density was calculated using Equation (3) for each hexagonal cell during each period.

$$\mathrm{DWRD}_j(r,f,m)=\frac{\mathrm{WRD}_{bj}-\mathrm{WRD}_{aj}}{\mathrm{WRD}_{bj}}, \quad (3)$$

where $DWRD_j$ is the increased local weighted road density at the *j*th hexagonal cell for the rural (*r*), forest (*f*), and mine (*m*) roads; WRD_{aj} and WRD_{bj} are the local weighted road density at the beginning and the end of the period at the *j*th hexagonal cell, respectively.

2.2.2 | Forest loss, fragmentation, and degradation

To obtain three dimensions of forest changes, that is, forest loss, fragmentation, and degradation, we used a variety of data to derive accurate forest areas in the four study times including aerial photos (scale 1:20,000) of 1966 and high-level USGS Landsat Surface Reflectance Climate Data Records products (USGS 2018) including Landsat 5 Thematic Mapper (August 10, 1987); Landsat 7 Enhanced Thematic Mapper Plus (July 20, 2000); and Landsat 8 Operational Land Imager (August 25, 2016). We selected the images with the highest quality and the lowest spectral interference of forest and other vegetation types such as grasslands and croplands. The aerial photos were registered using Landsat images and merged as a single photo for facilitating segmentation and object interpretation. We designed several rules to detect forest, non-forest, and forest-changed objects using OBIA (Dorren, Maier, & Seijmonsbergen, 2003; Navulur, 2006; Newman et al., 2014; Raši et al., 2013; Uddin et al., 2015; Willhauck, Schneider, Kok, & Ammer, 2000).

Forests in 1966, 1986, 2000, and 2016

Forest in 1966. We created two new channels[1] by conducting the sharpening and embossing filters on the aerial photos and then we combined them with the main layer to create a multispectral photo. Image segmentation was carried out with a scale value of 250 to delineate homogenous objects of forest and non-forest areas on the multispectral photo of 1966. Some segments were selected from the forest and non-forest objects as training data. To improve the accuracy of classification, we calculated a variety of ancillary features by comparing spectral and textural parameters such as brightness and textures derived from gray-level co-occurrence matrix, for example, mean, standard deviation, homogeneity, dissimilarity, contrast, entropy, and angle second moment (Eitzel et al., 2016; Halounová, 2003; Navulur, 2006). We optimized the large dimensions of the features to gain the best separation distance and dimension for classification. We applied the best result to the classes and then classified them using the standard nearest neighbor algorithm (Figure 2a).

Forest in 1986, 2000, and 2016. The rule-based classification using OBIA (Belgiu, Drăguţ{t\hskip-0.7ex\char "B8}, & Strobl, 2014; Lewinski, Bochenek, & Turlej, 2010; Ziaei, Pradhan, & Mansor, 2014) was applied to detect forest and non-forest classes within the Landsat 5, Landsat 7, and Landsat 8 images. We used multiresolution segmentation algorithm for the formation of segment objects from the Landsat images. The optimal scale parameters were determined by trial and error, with a higher weight for near-infrared (NIR) band and a higher value of compactness than shape. We defined land use features following the Level 2 of USGS classification system (Anderson, 1976) to obtain an accurate forest classification. After sampling, various ancillary features were generated with respect to the spectral, textural, and contextual properties of the multispectral images including the spectral features such as the mean, standard deviation (*SD*), brightness and maximum difference (max. diff.); vegetation indices such as green vegetation index (Aguilar et al., 2016) and enhanced vegetation index 2 (EVI2); the textural features derived from the gray-level co-occurrence matrix (e.g., mean, standard deviation, homogeneity, dissimilarity, contrast, entropy, and angle second moment); the contextual features such as the vicinity to the forest layer of the previous time; and topographic features such as slope. Following that, we determined the thresholds of the object features for each land-use class and examined a set of rules for extracting the forests of 1986, 2000, and 2016 (Figure 2b–d). The accuracy of forest layers was validated using provided ground truth samples and confusion matrix through user's accuracy, producer's accuracy, observed agreement, and kappa coefficient (Gómez, Biging, & Montero, 2008).

Forest loss

We calculated the rate of forest loss within each hexagonal cell for a particular time period using Equation (4) (Shirvani et al., 2017).

$$\mathrm{Fl} = \frac{\mathrm{Fa} - \mathrm{Fb}}{\mathrm{Fa} * T}, \tag{4}$$

where *T* is the total number of years for a particular time period, and F_a and F_b are the areas of the forest at the beginning and the end of the period, respectively.

Spatial autocorrelation indicators (Anselin, 1995) were used to examine whether spatial relationships shape the patterns of forest loss throughout the study area by the global Moran's *I* and within the cells by LISA. The output maps of LISA include the clusters that determine where cells with high rates of forest loss surrounded by each other (high–high) and where cells with low rates of forest loss are in the neighborhood of each other (low–low) and also the outliers that determine if a cell with a high rate of forest loss is surrounded by cells with low rates of forest loss (high–low) or a cell with a low rate of forest loss is surrounded by cells with high rates of forest loss (low–high).

Forest fragmentation

Forest patches were created by overlaying the road segments on the forest polygons of 1966, 1986, 2000, and 2016. The fragmentation rate of patches was calculated using three metrics including edge density, the average amount of edge per patch, and mean shape index (McGarigal & Marks, 1995) within the hexagonal cells for each study period. Following that, we used the global Moran's *I* and LISA (Anselin et al., 2006) to depict the clusters (high–high and low–low) and outliers (high–low and low–high) of forest fragmentation.

Forest degradation

Although some forests of the Hyrcanian region were not affected by direct driving forces of forest loss and forest fragmentation, they were

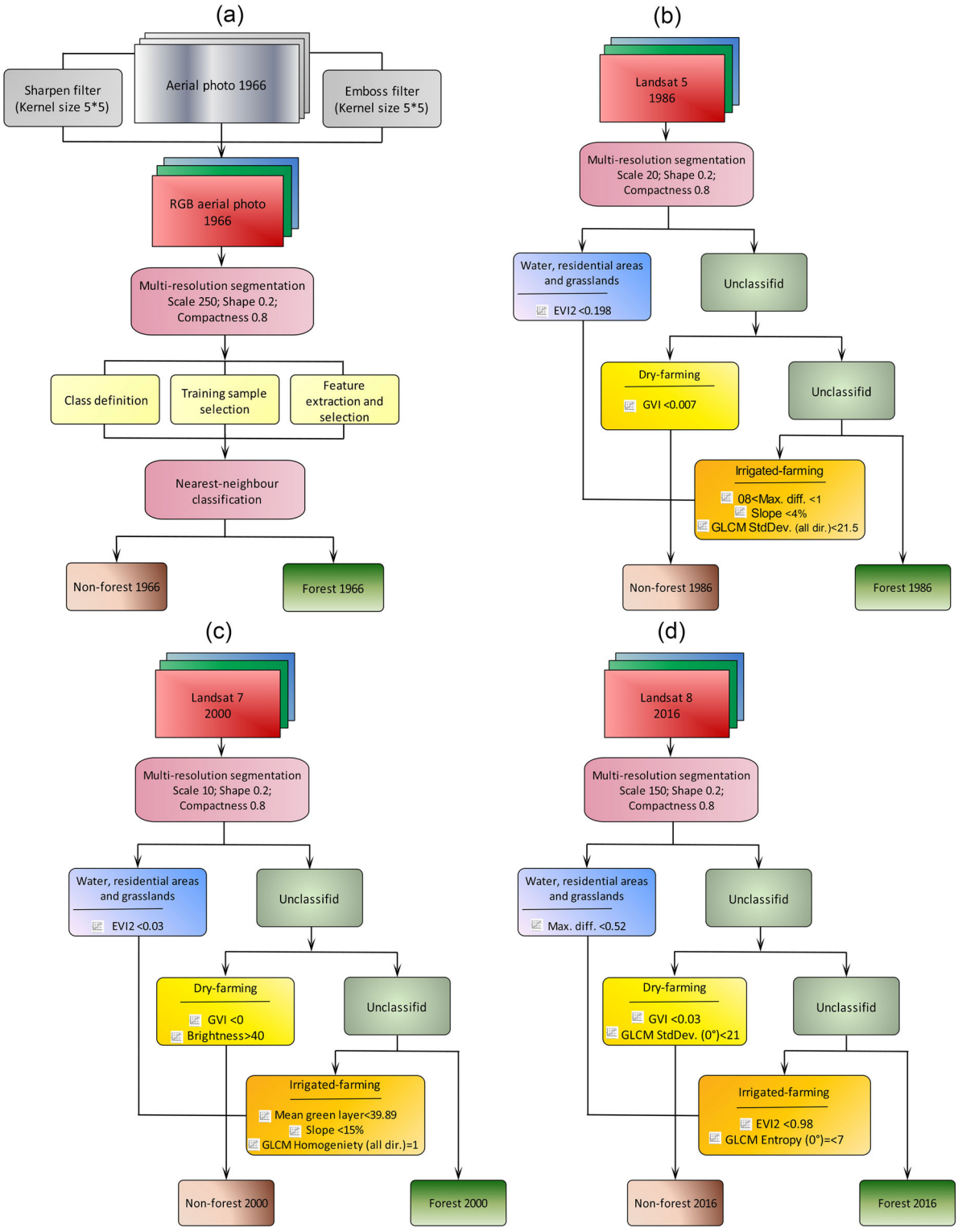

FIGURE 2 The workflows of forest extraction from (a) the aerial photos and object-based standard nearest neighbor classification for 1966 and the Landsat imagery and rule-based object-oriented classification for (b) 1986, (c) 2000, (d) and 2016 in northeast Iran. Abbreviations: EVI2, enhanced vegetation index 2; GLCM, gray-level co-occurrence matrix; GVI, green vegetation index; max. diff., maximum difference; stdDev., standard deviation [Colour figure can be viewed at wileyonlinelibrary.com]

degraded by intensive human activities such as timber harvesting, mining, and forest fires, which may decrease the density and quality of forest types. To address this issue, Landsat time-series images were analyzed from 1972 to 1986, 1987 to 2000, and 2001 to 2016. We selected the images obtained during August, September, or October of each year with the cloud cover less than 10%. Because the level of

correction of images was 1*T* in the first period, the radiometric and atmospheric corrections were applied on the Landsat images using dark-object subtraction technique (Chavez, 1988), and topographic correction was applied using C-correction approach (Teillet, Guindon, & Goodenough, 1982). Moreover, we masked all cloud and forest loss patches within the images for minimizing their effects on the time-series anomalies. We retrieved forest density using the EVI2 (Jiang, Huete, Didan, & Miura, 2008), calculated from NIR and red bands, for the selected month of each year (Equation 5). Then the degree of forest degradation was calculated for a specific year (X_i) in comparison with the mean (μ) and standard deviation (σ) of the forest density during the period using the *z*-scores distribution (Equation 6; Hald, 1952). The final forest degradation value was calculated as the median of *z* scores of total years within a cell during each period. The output values range between −4 and +4 as a higher negative value indicates a higher degree of forest degradation and a higher positive value indicates a higher degree of forest virginity.

$$\mathrm{EVI2} = 2.5 \times \frac{\mathrm{NIR} - \mathrm{Red}}{\mathrm{NIR} + 2.4 \times \mathrm{Red} + 1}. \quad (5)$$

$$z_i = \frac{X_i - \mu}{\sigma}. \quad (6)$$

2.2.3 | Spatiotemporal autocorrelation of road expansion and forest changes

The BiLISA (Anselin, Syabri, & Smirnov, 2002) was used to find the relationships between the expansion of road density at a period and its neighborhoods in a previous time period. Likewise, we analyzed the effects of forest changes in a period on the forest changes in the next period. The computation of bivariate local Moran's *I* is as follows:

$$I_B = \frac{\sum_i \left(\sum_j w_{ij} z_{(p-1)j} \times z_{(p)i} \right)}{\sum_i z^2_{(p)i}}, \quad (7)$$

where $z_{(p)}$ and $z_{(p-1)}$ are the standardized *z* scores of a period and the previous period, respectively. w_{ij} is the spatial weights matrix between the location *i* and its neighborhoods *j*, which is defined on the basis of the queen contiguity matrix with a first order of neighbor in a 3 × 3 matrix (Anselin & Rey, 2014; Cliff & Ord, 1973).

2.2.4 | Spatial relationships between forest changes and road density expansion

Spatial regression models were used to find associations between the magnitude of three dimensions of forest change and the expansion of the density of three road types during the three periods. The spatial lag and spatial error models are calculated using Equations (8) and (9) (Anselin & Rey, 2014), respectively.

$$Y = \rho W y + X\beta + u, \quad (8)$$

$$Y = X\beta + \lambda W + \varepsilon, \quad (9)$$

where *Y* is the rate of forest loss, forest fragmentation, or forest degradation for a period; *Wy* is the spatially lagged dependent variable with spatial coefficient ρ; *X* is the explanatory variables (weighted density of rural, forest, and mine roads) with coefficient β; and *u* is the term of errors in the spatial lag model, which is decomposed to the spatial lag of the errors with the spatial autoregressive parameter λ and a normal distributed error (ε).

We tested the existence of spatial dependence using the parameters of Lagrange multiplier statistics and Moran's *I* at the 95% confidence level (Anselin & Rey, 2014). Moreover, the superior spatial regression models were selected using the highest values of R^2 and the lowest values of Akaike information criterion from the comparison of the spatial models (Anselin & Rey, 2014).

3 | RESULTS

3.1 | Extraction of road networks

The density of rural roads increased from 3.64 m ha^{-1} in 1986 to 4.56 m ha^{-1} in 2000; however, it slightly decreased to 4.35 m ha^{-1} in 2016. The growth of population led to rural road development during the periods of 1966–1986 and 1986–2000; the annual population growth was approximately 7.07% and 2.12% during these time periods. The comparison of rural roads revealed that many of the paved and gravel roads were results from upgrading the the trail or gravel roads, especially in 1986 and 2000 (Figure 3). However, the road density decreased during the third period.

The density of forest roads and mine haul roads gradually increased from 1966 to 2016 (Figure 3). The number of logging plans increased from 10 in 1986 to 17 FMPs in 2016. Logging operations were implemented in 644 parcels (45,935 ha) during the period of 1966–1986, of which 178,671 m of forest road were constructed for transporting the logs to the market. Whereas, the number of logging areas reached 956 parcels (71,383 ha) in 2000, and about 260,893 m of new roads were established during this time period. Furthermore, the number of logging areas (1,159 parcels) slightly increased in 2016 as about 304,508 m of new roads were constructed over the FMPs during the third time period (Figure 3). Likewise, the development of mining plans remarkably increased the length of mine roads to 229,315 m in the second period and 436,826 m in the third period (Figure 3). The number of mine plans dramatically increased from 3 in 1986 to 29 plans in 2016.

3.2 | Changes in road density

The overall aggregate of average population density reveals that approximately 795 n ha^{-1} during 1966–1986, 1,446 n ha^{-1} during 1986–2000, and 1,753 n ha^{-1} during 2000–2016 were distributed

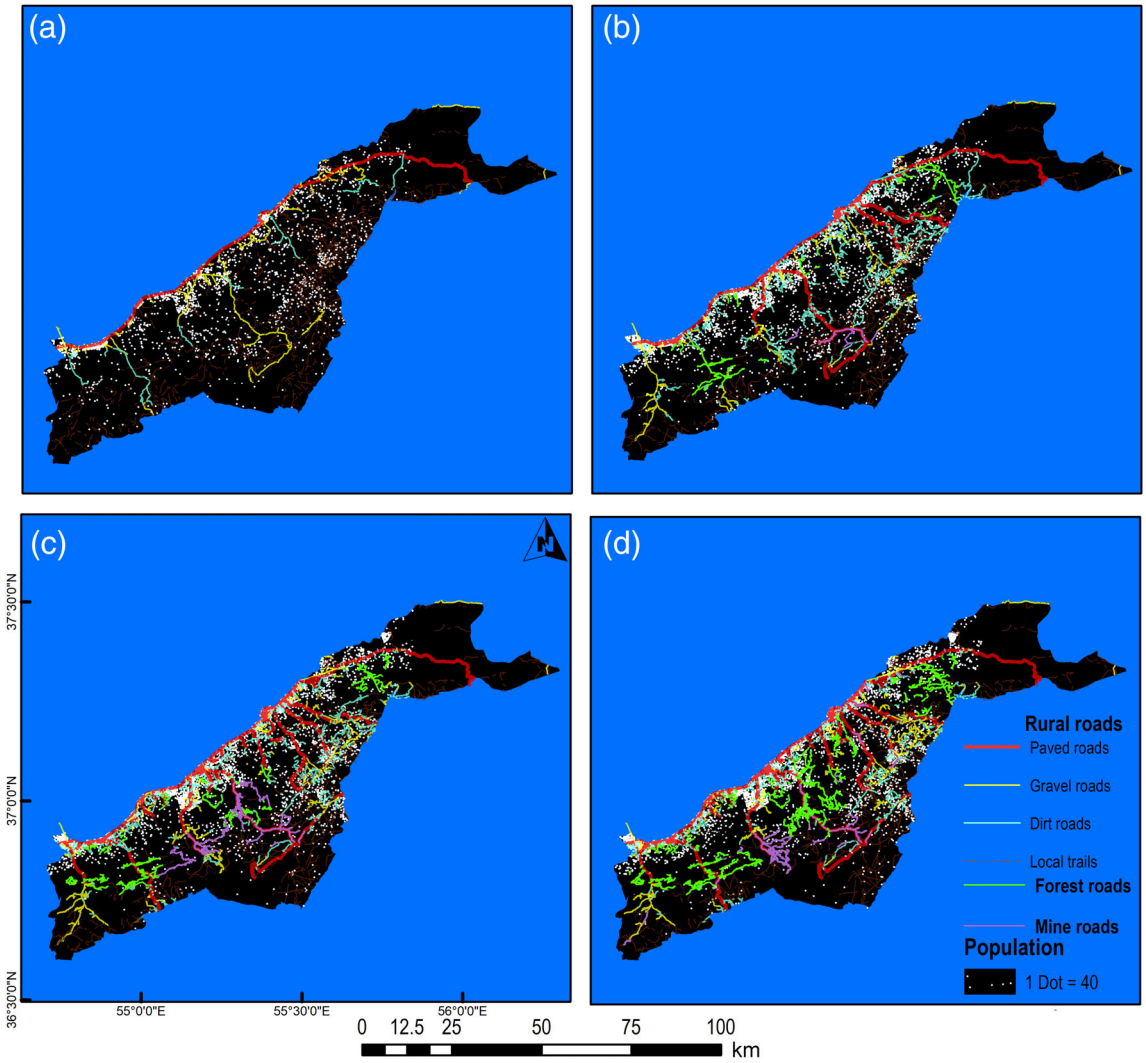

FIGURE 3 Rural roads are upgraded from low levels to the high levels from (a) 1966 to (b) 1986, (c) 2000, (d) and 2016. Unlike the cities, population density steadily decreased in the rural areas between 1986 and 2016 in northeast Iran. However, forest and mine roads increasingly expanded from (b) 1986 to (c) 2000 and (d) 2016 in northeast Iran [Colour figure can be viewed at wileyonlinelibrary.com]

along the rural roads. The spatial variation of weighted road density shows a decrease in population nearby villages from 1966 to 2016 and a significant increase in population nearby cities during the periods of 1986–2000 and 2000–2016 (Figure 4). The number of cities increased from four in 1966 to nine in 2016, which led to the development of the rural roads from 565 to 1,898 km during the study time. In contrast, the length of trail roads decreased from 2,062 km in 1966 to 1,365 km in 2016. The majority of villages was using the trail roads, particularly, over the central and southern parts of the study area during the beginning of 1966–1986 (Figure 4a); as a higher population density was recorded across the trail roads in this time period in comparison with the second and third time periods (Figure 4d,g).

The spatiotemporal variations of the weighted density of forest roads indicated that the average of logging volume of parcels within the OCA of roads was higher than the parcels out of the OCA of roads during the second and third time periods, unlike the first time period (Figure 4). The highest difference value was obtained during the third time period by an average of 27.71 m^3 ha^{-1} in the parcels within the OCA, which was about 9.81 m^3 ha^{-1} higher than the parcels out of the OCA of roads (Figure 4h). The average of logging volume was about 27.75 m^3 ha^{-1} in the parcels within the OCA of roads, which was about 5.07 m^3 ha^{-1} higher than other parcels during the second time period (Figure 4e). However, the average of logging volume in the parcels out of OCA of forest roads (12.41 m^3 ha^{-1}) was higher than the parcels in OCA of the roads (7.78 m^3 ha^{-1}) during the first period (Figure 4b). Likewise, the spatiotemporal variations of the weighted density of mine roads show that the average of mining extraction in the OCA of mine roads was remarkably higher than the plans out of the OCA of roads during three time periods (Figure 4c,f,i). The average of mining extraction was obtained: 858, 1,037.7, and 1,811.54 t ha^{-1} out of the OCA of mine roads; and 2,503, 2,920.86, and 3,144.2 t ha^{-1} in the OCA of the roads over three time periods, respectively.

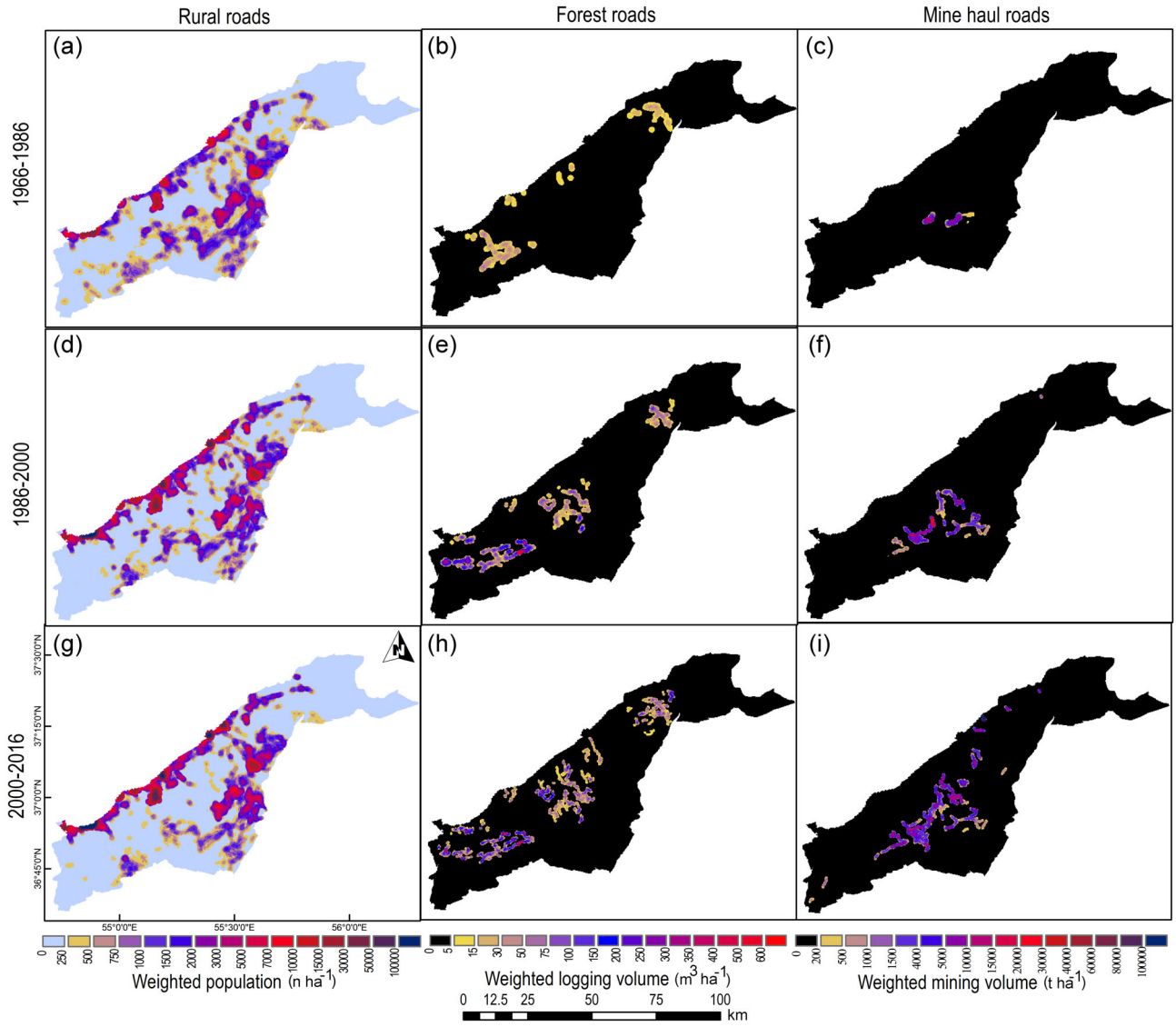

FIGURE 4 Weighted density of the rural roads from (a) 1966–1986 towards (d) 1986–2000 and (g) 2000–2016 has decreased; however, the weighted density of forest roads and mine haul roads from (b,c) 1966–1986 towards (e,f) 1986–2000 (h,i) and 2000–2016 has been increased in the eastern part of Hyrcanian forests [Colour figure can be viewed at wileyonlinelibrary.com]

3.3 | Changes in forests

3.3.1 | Forest loss

The results of image classification showed that the object-based approaches performed satisfactory accuracy for discriminating forest from non-forest objects either by aerial photos in 1966 or Landsat images from 1986 to 2016 (Table 1). The comparison of forest areas revealed that the rates of forest loss decreased from 1966 to 2016 in northeast Iran: about 20,973 ha during 1966–1986; 17,678 ha during 1986–2000; and 6,258 ha during 2000–2016. Forest loss showed significant spatiotemporal autocorrelation (p value < .05) by I = .662, I = .674, and I = .557 in the three time periods, respectively. The clusters with high rates of forest loss (high–high) are distributed in the northern parts of the region nearby the population centers and roads during the first time period (Figure 5a). These clusters extended to the central and southern parts of the forests during the second period (Figure 5d), with higher concentration in the southern parts during the third period (Figure 5g). Moreover, spatiotemporal correlation was significant between forest losses during the second period and the first period (I_B = .246, p value < .05). Figure 6a depicts that the high–high clusters of forest loss in the second time period are formed in the neighborhoods of forest loss areas in the first time period. Likewise, the clusters of forest loss in the third time period were in the neighborhoods of the high–high cluster in the second time period (I_B = .461, p value < .05). There are some scattered areas with a high rate of forest loss during the third time period that have received a low rate of forest loss during the second time period (high–low) in the western and southern parts of the study area (Figure 6d).

TABLE 1 Accuracy assessment results of object-based classification of forest and non-forest categories using aerial photos and Landsat images in northeast, Iran

Metric	Category	User's accuracy				Producer's accuracy			
Time		1966	1986	2000	2016	1966	1986	2000	2016
Method		NN	RB	RB	RB	NN	RB	RB	RB
Category	Forest	0.8102	0.9423	0.9245	0.96	0.9911	0.9608	0.9608	0.9320
	Nonforest	0.9841	0.9583	0.9574	0.93	0.7045	0.9388	0.9184	0.9588
Observed agreement		0.865	0.95	0.94	0.945	–	–	–	–
Kappa coefficient		0.7175	0.8999	0.8798	0.89	–	–	–	–

Note: NN, nearest neighbor classification; and R, rule-based classification using object-based image analysis.

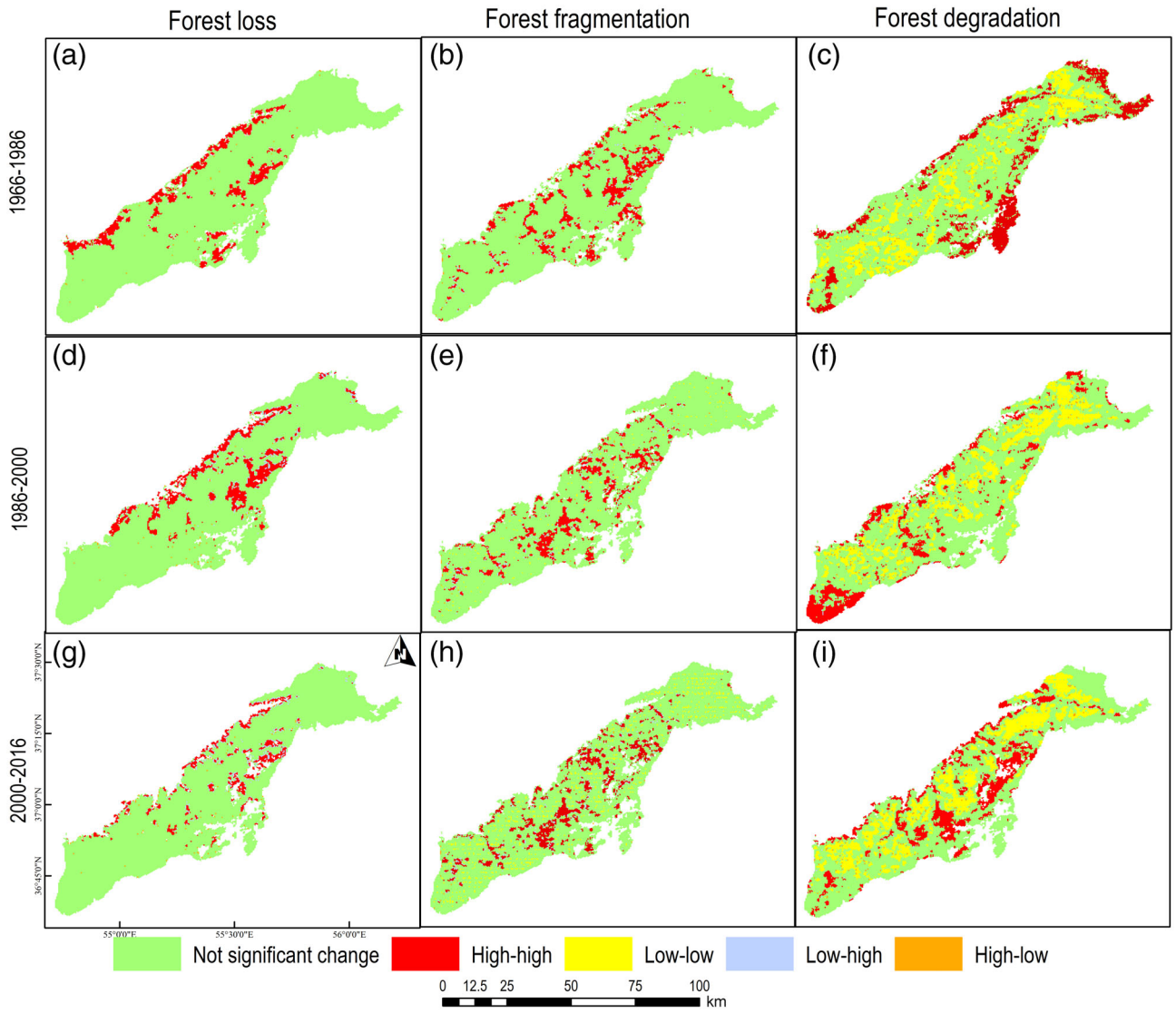

FIGURE 5 Spatial patterns of forest loss show that the trend of forest loss has decreased from (a) 1966–1986 and (d) 1986–2000 towards (g) 2000–2016 in Hyrcanian forests. However, the scatter of forest fragmentation is broader in the (h) third time period in comparison with the (e) second and the (b) first time periods. Likewise, multiple high–high clusters of forest degradation emerged in the heart of the forest in the time period (i) 2000–2016 in comparison with the time periods (f) 1986–2000, and (c) 1966–1986 [Colour figure can be viewed at wileyonlinelibrary.com]

3.3.2 | Forest fragmentation

The analysis of classified forest patches indicated that the rate of forest fragmentation has significantly increased from 1966 to 2016. The number of forest patches has increased from 667 patches in 1966 to 1,086 patches in 2016; the average area of forest patches declined from 521 to 273 ha; and the average length of edges has increased from 4.6 to 5.6 km. High–high clusters of fragmented forests are

distributed in the central parts of the study area during 1966–1986, which extended to the western parts during 1986–2000, and throughout the region—except the protected area in the east—during 2000–2016 (Figure 5b,e,h).

The rate of forest fragmentation showed a significant positive correlation in the second and third time periods with their neighborhoods in the first (I_B = .351, p value < .05) and second (I_B = .4746, p value < .05) time periods. However, there are some locations with a high rate of fragmentation in a upper time period and low rate of fragmentation of their neighborhoods in the lower time period (high–low), which indicate the temporal increase of forest fragmentation in the study area (Figure 6b,e).

3.3.3 | Forest degradation

The rate of forest degradation has increased from 1966 to 2016. The average rates of forest degradation obtained 3.18%, 4.6%, and 7.0% during the three time periods, respectively. Moreover, spatiotemporal patterns of forest degradation showed a significant positive autocorrelation in the three time periods (I = .611, I = .608, and I = .634). Although the high–high clusters of forest degradation are distributed at the margins of forests (Figure 5c), they have emerged at the heart of the forests during the second and third time periods (Figure 5f,i).

3.4 | Spatiotemporal autocorrelation of road expansion and forest changes

Spatiotemporal autocorrelation of forest degradation showed a significant negative correlation between the time periods of 1986–2000 and 1966–1986 (I_B = −.0209, p value < .05) unlike 2000–2016 and 1986–2000 (I_B = .0720, p value < .05). Although there are some locations with high–high clusters, the number of locations with high rates of degradation during 1986–2000 and low rates of degradation in their neighborhoods during 1966–1986 indicates the increase of forest degradation during 1986–2000 (Figure 6c,f).

3.5 | Spatial relationships of forest changes and road density expansion

The diagnostic tests for spatial dependence show that there are significant spatial relationships between three dimensions of forest changes and the expansion of three types of roads in the three study time periods (Table 2). Lagrange multiplier indicates that spatial error was the superior model to describe forest loss induced by the expansion of roads during 1966–1986 and 1986–2000, and forest fragmentation and forest degradation were affected by the expansion of roads in the three time periods. On the other hand, spatial lag shows higher performance than the spatial error in expressing forest loss induced by the expansion of roads during 1986–2000 and 2000–2016 (Table 3a).

Although the expansion of rural (ß = .030), forest (ß = .066), and mine (ß = .108) roads significantly (p value < .01) affected forest loss during the second time period, only rural road (ß = .131) shows significant coefficient in the first time period (Table 3a). There is no significant relationship (p value > .05) between forest loss and the expansion of the three road types in the third time period (Table 3a).

The expansion of forest roads was a significant variable in intensifying forest fragmentation during the three time periods (Table 3b). The coefficients of forest road have remarkably increased from the time period of 1966–1986 (ß = .057, p value < .05) to 1986–2000 (ß = .096, p value < .05) and 2000–2016 (ß = .306, p value < .01). Moreover, the coefficients of mine road were positive and significant during 1986–2000 (ß = .049, p value < .05) and 2000–2016 (ß = .177, p value < .01). The expansion of rural road was only significant on the fragmentation of forests during 1966–1986 (ß = .049, p value < .01; Table 3b).

The coefficients of mine road were positive in expressing forest degradation during the three time periods; however, strong effects were recorded during 1986–2000 (ß = .224, p value < .01) and 2000–2016 (ß = .109, p value < .01). Likewise, the coefficients of rural road were positive and significant (p value<.01) during 1966–1986 (ß = .766) and 1986–2000 (ß = .167), but the expansion of forest roads was only significant on the forest degradation during 1986–2000 (ß = .110, p value < .01; Table 3c).

4 | DISCUSSION

4.1 | Upgrading rural roads and expanding forest and mine roads

The results of road changes show that the density of rural roads gradually declined from 1966 to 2016 (Figure 4). Some relocation efforts led to a decline in the population of rural areas, causing a decrease of road density during 2000–2016; some villages were destroyed because of the devastating flood of 2001 in the east of the study area, which the government decided to resettle inhabitants to the new remote complex villages from the forest areas (Japan International Cooperation Agency, 2006). Furthermore, the conservation plans of removing livestock from the forests have been implemented over all the villages by less than 20 households or dispersed single households in the forest areas since 2002 (Rezaee & Moayeri, 2014). However, the density of forest roads and mine haul roads sharply increased especially during 1986–2016 (Figure 4). The traditional systems such as horse and mule logging were extensively used for skidding logs throughout the Hyrcanian forests during 1966–1986. Logging operations were sporadically conducted depending on the small-scale timber harvesting methods in the FMPs; as this system is less dependent on the dense road networks, therefore, forest road networks were less developed (Figure 4b). Since the 1980s, the system of timber

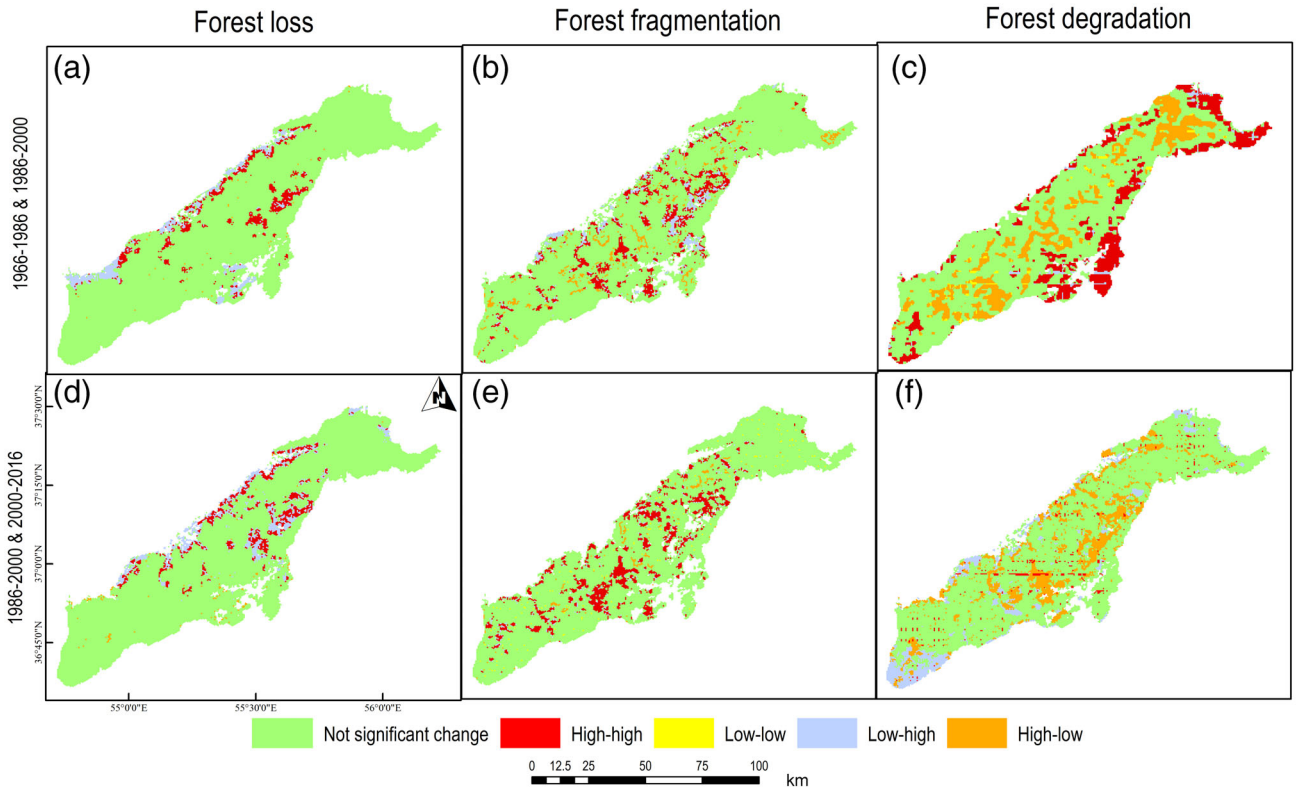

FIGURE 6 Spatial patterns of forest loss show that high–high clusters in (a) the time period 1986–2000 are surrounded by the same clusters in the time period 1966–1986 as well as in (d) the time periods 2000–2016 and 1986–2000. Likewise, significant positive spatial correlations occurred between forest fragmentation in (b) the time periods 1986–2000 and 1966–1986 as well as between (e) 2000–2016 and 1986–2000. Prevalence of high-low outliers of forest degradation between (c) 1986–2000 and 1966–1986 indicates the expansion of forest degradation trend throughout the Hyrcanian forests [Colour figure can be viewed at wileyonlinelibrary.com]

harvesting has gradually converted from animal power to a mechanized method; as the density of forest roads has been increased in the FMPs; therefore, parcels in neighborhoods of the roads recorded higher volumes of logging, particularly during 2000–2016 (Figure 4e, h). Despite the current government's actions for mitigating the intensive timber harvesting in the Hyrcanian forests, the construction of forest road networks has been accelerating during the recent decades. The logging operations have intensified along with the development of the forest roads with a higher density in the western and eastern parcels of the study area (Figure 4h). Moreover, skidding trails were developed for skidding logs in the locations with a weak coverage of forest road network during the third period. Ample damage induced by skidding trails to the seedlings, residual trees, and soil compaction has been reported throughout the world (Buckley, Crow, Nauertz, & Schulz, 2003; Cudzik, Brennensthul, Białczyk, & Czarnecki, 2017; Gullison & Hardner, 1993; Modrý & Hubený, 2003; Tsioras & Liamas, 2015), as well as in the Hyrcanian forests (Badraghi et al., 2015; Jamshidi, Jaeger, Raafatnia, & Tabari, 2008; Jourgholami, 2012).

Furthermore, the mechanization of mining has increased the operations and mine haul roads in the forest areas of northeast Iran. Although the legislation of eliminating destructive development schemes in the forests was ascertained by the parliament, the exploration and development of some mine types such as coal and dimension stones were predestined with the discretion of the Iranian Department of Environment (Islamic Consultative Assembly of Iran, 2003). The underground and open-cast mining are both increasing. For example, the active sites of underground coal mines have increased from 6 in 2000 to 16 sites in 2016 due to their profitability in providing employment and fossil fuels by the organization of industry, mines, and trade of the Golestan Province. Likewise, the open-cast mines have been increased for mining limestone and gravelly materials, for example, the Nilkooh limestone mine in the southeast of the study area (Figure 7).

4.2 | Declining forest loss and increasing forest fragmentation and degradation

The trend of spatial patterns of forest changes has been changing from forest loss in the past decades to forest fragmentation and forest degradation in the recent decades in the Hyrcanian forests, northeast Iran. Forest loss has been centralized along the population centres in the lowland verges during the first and second time periods (Figure 5a,d). The residential growth rate was annually about 10% and 2% in the rural and urban areas, respectively; the population has increased from 94,200 inhabitants in 1966 to 299,700 inhabitants in

TABLE 2 The values of the tests of diagnosing of spatial dependency and selecting the robust model

Variable	1966–1986			1986–2000			2000–2016		
	FL	FF	FD	FL	FF	FD	FL	FF	FD
Moran's *I* (error)	0.3978**	0.2299**	0.4993**	0.8705**	0.2034**	0.4460**	0.4450**	0.2036**	0.5158**
Lagrange multiplier (lag)	975.7629**	463.0420**	816.63**	3,497.675**	408.7993**	1,143.987**	487.920**	409.0349**	2,462.7768**
Robust LM (lag)	0.0347^{ns}	3.9909*	2.47^{ns}	375.2454**	0.6825^{ns}	6.877**	0.6836**	20.0202**	0.2694^{ns}
LM (error)	976.9805**	465.2380**	814.16**	3,176.437**	409.9448**	1,154.822**	487.715**	426.1948**	2,462.7161**
Robust LM (error)	1.2523*	6.1869**	0.0025^{ns}	54.0075**	1.8281*	17.7118**	0.4778**	37.1801**	0.2086^{ns}
Conclusion	SE	SE	SL	SL	SE	SE	SL	SE	SL

Abbreviations: FD, forest degradation; FF, forest fragmentation; FL, forest loss; ns, not significant; SL, spatial lag; SE, spatial error.
**p value < .01; *p value < .05.

2000 (Statistical Center of Iran, 1966; 1986; 1996; 2011; 2016). Sprawling in residential areas and expanding of farmlands were reported as the main driving forces of forest loss in northeastern Iran (Shirvani et al., 2017). In the forested area, the annual rate of forest loss was obtained about 0.3% in 1966–2000, which was less than the annual rate of deforestation of 0.85 that reported by Shirvani et al., 2017 for the entire basin, as its population density and residential growth were lower than the entire basin during this period of time. In 2000–2016, forest loss declined approximately 70% and 65% in comparison with the forest loss during 1966–1986 and 2000–2016; BiLISA maps confirm that spatial patterns of forest losses are significantly correlated between 1986–2000 and 1966–1986 (Figure 6a) and 2000–2016 and 1986–2000 (Figure 6b). The primary causes for the decline of forest loss are the evacuation of some indigenous inhabitants from the forests to the established new counties and the dispossession of the majority of livestock holders from the forests and montane grasslands towards semi-steppe grasslands during the last period (Abdi, Shirvani, & Buchroithner, 2018).

Although the trajectory of forest loss is declining in 2016, forest fragmentation and forest degradation are increasingly growing due to the proliferation of development projects and infrastructure in the pristine forests. Since the 1980s, timber harvesting and mining have been rapidly growing and then forest road and mine haul road networks have been expanding, which penetrated the heart of forests for transporting logs and mineral materials. In the second and third periods, the average of logging was 2.8- and 1.8-times higher than the average of logging in the first period in the FMPs (Figure 4b,e,h). Moreover, the average of mineral exploration of these two periods was 2.04- and 9.2-times higher than the first period in the mining plans (Figure 4c,f,i).

The continuous areas of forests have been breaking up into smaller segments from 1966 to 2016, as the proportion of segments in 2016 is 1.63-times of the forest segments in 1966. The high rates of forest loss and the expansion of the rural roads increased the forest edges at the end of the first time period, as about 11.56% of the forests are falling into the high–high cluster of fragmentation in 1986 (Figure 5b). Following that, the development of logging and mining projects caused proliferation of forest roads and mine haul roads within pristine forests as well, which led to increasing high fragmentation areas to 11.30% and 11.40% in 2000 and 2016, respectively (Figure 5e,h). The protected areas—with the minimum amount of road development—showed a few significant values of high–high fragmentation (Hawbaker, Radeloff, Clayton, Hammer, & Gonzalez-Abraham, 2006; Newman et al., 2014) over all time periods; a good example of less fragmented protected area is the Golestan National Park in the northeast of the study area (Figure 5b,e,h).

In 1966–2000, high forest degradation (high–high) is distributed in the southern and western verges of forests where they are adjacent to the rangelands, therefore, the overgrazing of livestock was likely one of the main causes of the high degradation in these parts of the forests (Figure 5c,f). Although the rate of degradation significantly decreased by removing livestock within the forests and rangelands plans in the third time period (Figure 5(i)), mining operations have started from the central forests since the period 1966–2000 (Figure 4c) and have been

TABLE 3 Spatial relationships between the standardized rates of (a) forest loss, (b) fragmentation, and (c) degradation with the expansion of rural, forest, and mine roads

(a)	1966–1986			1986–2000			2000–2016		
Variable	OLS	LS	SE	OLS	LS	SE	OLS	LS	SE
Constant	0.0632^{ns}	−0.0137^{ns}	−0.0526^{ns}	1.9217**	0.5223**	1.0047**	−0.0230^{ns}	−0.0272^{ns}	−0.0419^{ns}
Rural road	0.1010**	0.06315**	0.1309**	0.1776**	0.0307**	0.0089*	0.0083^{ns}	−0.0027^{ns}	−0.0113**
Forest road	0.0687*	0.0305^{ns}	0.0561^{ns}	0.5407**	0.0666**	0.0134	-	-	-
Mine road	−0.1853*	−0.0545^{ns}	0.0050^{ns}	0.1454^{ns}	0.1083**	0.1058**	−0.0164^{ns}	−0.0127^{ns}	−0.0170^{ns}
λwy	-	0.4988**	-	-	0.9002**	-	-	0.4562**	
Lambda (εwv)	-	-	0.5050**	-	-	0.9195**	-	-	0.45642**
R^2	0.0124	0.2789	0.2825	0.0717	0.9271	0.9354	0.0001	0.2732	0.2734
AIC	11,169.4	10,270.6	10,258.3	8,284.45	2,131.98	1913.29	5,248.59	4,819.48	4,817.26
(b)									
Constant	−0.0110^{ns}	−0.0300*	−0.0466**	1.5808**	1.0788*	1.4599**	0.18904**	0.13202**	0.1771**
Rural road	0.0433**	0.0342**	0.0493**	−0.0261*	−0.0208^{ns}	−0.0264^{ns}	−0.0194^{ns}	−0.0167^{ns}	−0.0205^{ns}
Forest road	0.0909*	0.0725*	0.0570*	0.0463^{ns}	0.0366^{ns}	0.0963*	0.2789**	0.2234**	0.3062**
Mine road	0.0477^{ns}	0.0403^{ns}	−0.00001^{ns}	0.00001**	0.00001**	0.0486*	0.1383*	0.1155*	0.1769**
λwy	-	0.2948**	-	-	0.2703**	-	-	0.2637**	-
Lambda (εwv)	-	-	0.2961**	-	-	0.2712**	-	-	0.2713**
R^2	0.0040	0.0977	0.0986	0.0149	0.0909	0.0913	0.0277	0.0995	0.1031
AIC	16,433.2	15,972.5	15,967.2	18,031.9	17,669.1	17,665.4	18,587.1	18,226.6	18,207.1
(c)									
Constant	−0.1162*	−0.0346^{ns}	−0.1174^{ns}	0.1631**	0.0740*	0.1343*	0.0436^{ns}	0.0272^{ns}	0.0662^{ns}
Rural road	0.5814**	0.2675**	0.7669**	0.1353**	0.0823**	0.1675**	0.0261^{ns}	−0.0011^{ns}	−0.0092^{ns}
Forest road	−0.1242**	−0.0393^{ns}	−0.0754^{ns}	0.0655**	0.0393*	0.1102**	−0.0316^{ns}	−0.0041^{ns}	0.00026^{ns}
Mine road	0.2280**	0.0699^{ns}	0.1067^{ns}	0.1584**	0.1051**	0.2244**	0.0685*	0.0448*	0.1095**
λwy	-	0.6594	-	-	0.5350**	-	-	0.6567**	-
Lambda (εwv)	-	-	0.6624**	-	-	0.5464**	-	-	0.6572**
R^2	0.0505	0.4510	0.4519	0.0211	0.3276	0.3352	0.0022	0.4302	0.4307
AIC	4,877.33	4,206.44	4,204.23	9,925.08	8,940.46	8,914.92	13,071.7	11,087.3	11,082.2

Abbreviations: AIC, Akaike information criterion; ns, not significant; OLS, ordinary least squares; SE, spatial error; SL, spatial lag.
*p value < .05; **p value < .01.

extended steadily and continuously to the western and eastern parts of the study area during 2000–2016 (Figure 4i). Roughly 28% of the underground mine areas are directly located in the high–high clusters of degradation, and about 18% of them are in the low–low clusters during 2000–2016. Moreover, about 60% and 40% of the open-cast mine areas fall into the high–high and low–low clusters of degradation in this time period (Figure 8). However, some high–high clusters of forest degradation do not fall into the mining sites in the southeast of the study area, they are surrounded by the rural areas that are providing workforces for the mining and logging operations. Also many of these workforces are involve in other activities such as traditional farming and stock raising in the frontiers of the forests and mining plans. This finding is consistent with the earlier studies that showed forests are cleared for material extractions or degraded for infrastructure development in developing countries (Alvarez-Berríos & Aide, 2015; Bebbington et al., 2018; Butsic et al., 2015; Sonter et al., 2017). The high number of requests for and approvals of mining concessions is a serious threat for the degradation of the remaining pristine areas of Hyrcanian forests. As some recent research have pointed to mining expansions as the real risk for the protected areas and indigenous territories in the forest ecosystems (Bebbington et al., 2018; Butt et al., 2013; Potapov et al., 2017; Sonter et al., 2017). Furthermore, forest degradation is significant in the parcels that were affected by timber harvesting, though the class of degradation is dominated by the low–low cluster, intensive logging can modify these areas into the high–high cluster in the future. Moreover, the overlaps between logging and mining operations created extensive forest degradation (high–high) during 2000–2016 (Figure 8). However, the protected areas recorded few high values of degradation (Hawbaker et al., 2006; Newman et al., 2014) in small portions, which indicate that the development projects such as mining and logging significantly increased high values of degradation in the unprotected areas of Hyrcanian forests (Figure 8). Nevertheless, logging and mining operations were extended to the frontier or even inside the protected areas during 2000–2016 (Figure 8).

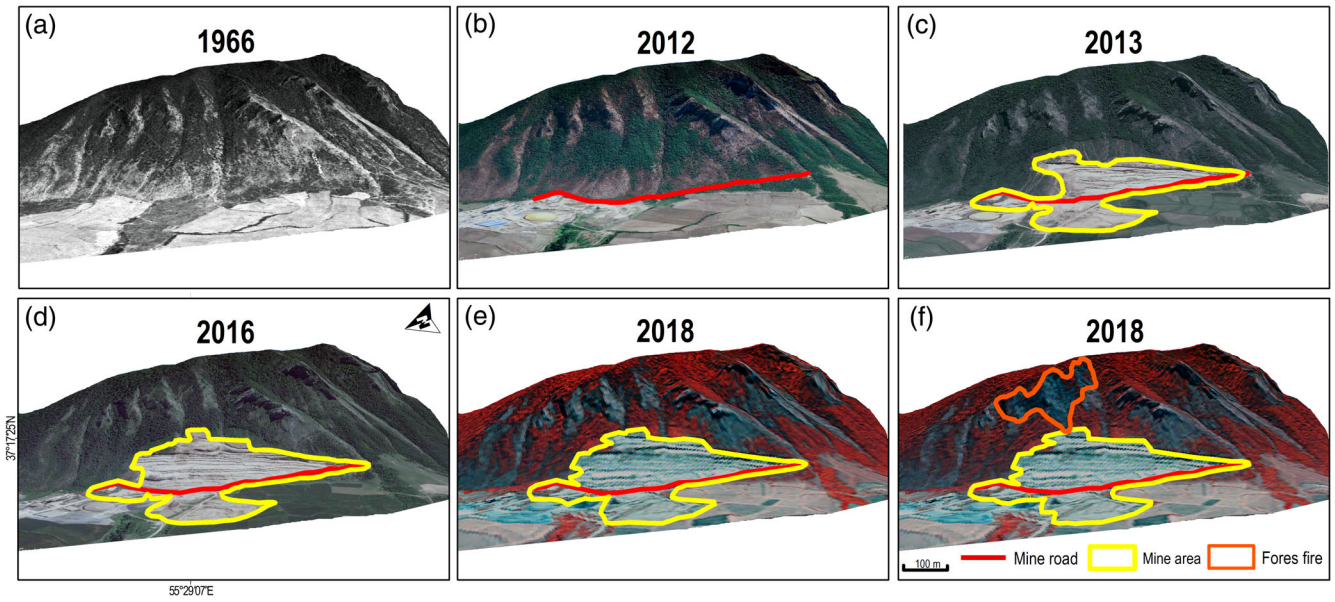

FIGURE 7 Intensified limestone extraction by the strip mine of Nilkooh has accelerated forest loss and forest degradation in northeast Iran (about 3 km away from Galikesh City): the aerial photo shows that the hillside of the mountain was covered by natural forests in (a) 1966; the factory of Peyvand Golestan Cement was established near to the Nilkooh mount in 2003 and mining operations and road construction have been started since (b) 2011–2012; about 16 ha of forest removed for mining in (c) 2013; the mining area expanded to 22.43 and 23.82 ha in (d) 2016 and (e) 2018; and the mine blasting ignited forest fire in (f) July 17, 2018 and burned about 9.7 ha of the adjacent forests [Colour figure can be viewed at wileyonlinelibrary.com]

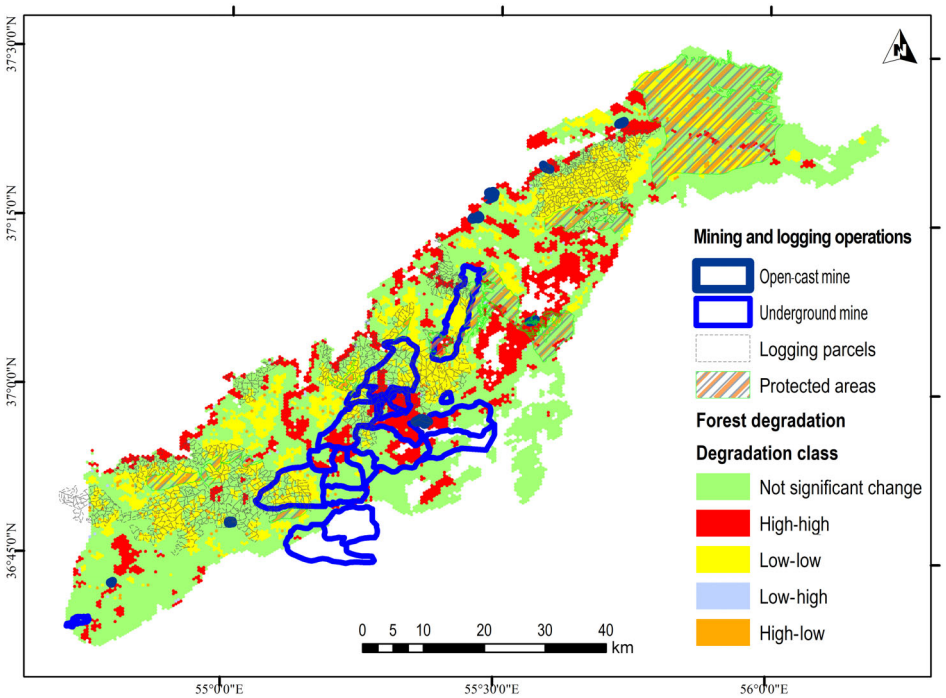

FIGURE 8 In the period 2000–2016, the operations of underground and open-cast mining caused significant high values of forest degradation within the mines' explorations and beyond the mines; logging operations caused low but significant forest degradation within the parcels; locations with overlaps of mining and logging operations received high values of degradation; protected areas received low degradation unlike the unprotected areas [Colour figure can be viewed at wileyonlinelibrary.com]

4.3 | Different impacts of low-volume road types on the forest loss, fragmentation, and degradation

We found that the dense rural roads entailed severe forest loss and forest degradation in the northeast Iran particularly between 1966 and 2000. However, its coefficient is positive but not significant during 2000–2016 (p value > .05). In the second and third periods, although the average population density was 1.82- and 2.31-times of the first period along the rural roads, the spatial variations of population show that the density of population steadily moved from the forest areas towards the vicinity of cities in the second and third periods (Figure 4a,d,g). Hence, the expansion of rural roads facilitated access

by follow on population for shifting forest to croplands and pastures and illegal logging by the consequences of significant forest loss and forest degradation (Ali et al., 2005; Barber et al., 2014; Jusys, 2016; Laurance et al., 2002; Mena et al., 2017) in the optimal area of the rural roads from 1966 to 2000. However, the expansion of rural roads steadily continued during 2000–2016, and declining population density within the forest areas caused lower weight values along the rural roads; therefore, three dimensions of forest changes showed no significant relationships with the expansion of rural roads in this period of time (Table 3). These results support our argument that the allocation of weight values for road segments in their optimal area has higher efficiency than the calculation of road distance in the entire study area, which was applied by earlier studies (Barber et al., 2014; Heilman et al., 2002; Jusys, 2016; Laurance et al., 2002; Mena et al., 2017; Riitters et al., 2000) for modeling spatial impacts of road expansion on deforestation and forest degradation.

Although forest roads showed the highest impacts on the forest fragmentation from 1966 to 2016, their impacts on the forest loss and forest degradation were merely significant during 1986–2000 (Table 3). With the expansion of logging concessions and mechanizations over the 1980s, the rates of timber harvesting and forest road construction accelerated within the natural forest stands focused on high-growing stock commercial tree species in the Hyrcanian forests. The length of forest roads increased from 178 km in 1986 to 439 km in 2000 and 744 km in 2016 throughout the study area. In addition, the rates of logging heightened from 0.62 m^3 ha^{-1} yr^{-1} in 1966–1986 to over 1.62 m^3 ha^{-1} yr^{-1} in 1986–2000 and 1.19 m^3 ha^{-1} yr^{-1} in 2000–2016 (Figure 4b,e,h). Likely, some logging operations such as clear-cutting and partial cutting along with intensive logging (1.98 m^3 ha^{-1} yr^{-1}) within the optimal area of roads increased forest loss and forest degradation during 1986–2000 (Figure 4e). However, changing timber harvesting system to selective logging decreased the rates of deforestation and forest degradation associated with logging and road building during 2000–2016, but its demand for a maximum coverage area by road network has significantly intensified road building and forest fragmentation in the northeast Iran. A number of studies verified significant forest loss, fragmentation, or degradation induced by the expansion of road networks within the forest ecosystems (Ali et al., 2005; Barber et al., 2014; Hawbaker et al., 2006; Mena et al., 2017; Newman et al., 2014). Nevertheless, it is important to distinguish between the intensity of these three dimensions of forest dynamics resulting from the expansion of forest roads or other road types.

The development of underground and open-cast mines increasingly expanded the length of mine roads from about 40 km in 1986 to over 435 km in 2016 within these forests. The expansion of mine roads was significant on forest loss, fragmentation, and degradation in the optimal areas of the roads since 1986 (Table 3b,c); however, its impact was continued on the forest loss only until 2000 (Table 3a). These road types are proliferated from the nearest rural roads and facilitated access by follow on population for shifting forest to croplands and illegal logging. As we discussed in the previous section, the significant forest fragmentation and degradation are occurring due to the underground and open-cast mining operations (Figure 8) with the most terrifying intensification in the optimal areas of the mine roads (Table 3b,c). However, sprawling open-cast mines are less than underground mines in these forests, as they created massive deforestation and forest fires, destruction of the forest landscape, for instance, the Nilkooh mine (Figure 7), soil erosion and deposit of a large amount of sediments into rivers, and pollution of the water table (Bell & Donnelly, 2014; Miranda et al., 2003). A small-scale intensified strip mining has increasingly created significant forest loss and forest degradation in developing countries (Asner et al., 2013; Bebbington et al., 2018). Coal mines are the dominant type of underground mines in the study area. Although the destructive impacts of underground mines may be less than the open-cast mines, a variety of damages resulting from these operations is reported in the forest ecosystems such as the subsidence after collapsing the mine, contamination of the air and climate resulting from a huge amount of waste, disturbance of the groundwater and streamflow due to decreasing the water table (Bell & Donnelly, 2014; Miranda et al., 2003), and biodiversity loss (Butt et al., 2013).

5 | CONCLUSIONS

With the contribution of time-series remote sensing data, OBIA, and spatial regression models, we developed a new analysis approach to retrieve 50-year variations of forest loss, fragmentation, and degradation caused by the expansion of rural, forest, and mine roads in northeast Iran. From this approach, we drew several conclusions. Though the expansion of rural roads has decreased, low-grade roads have been upgrading to higher grades. However, forest and mine roads have been expanding along with the mechanization and development of timber harvesting and mining operations since the 1980s in the Hyrcanian forests. Besides, the spatial variations of forest dynamics have been changing from forest loss in the past decades to forest fragmentation and degradation in recent decades throughout these forests. By the evacuation of population and livestock holders from the forest areas towards remote locations, the trajectory of forest loss has diminished. However, intensification of logging and mining operations have increasingly heightened the rates of forest fragmentation and degradation in the pristine forests since the 1980s. Specifically, the low-volume road types have different impacts on the forest loss, fragmentation, and degradation over the three time periods. The expansion of rural roads was significant on the high rates of forest loss and fragmentation until 2000, and the proliferation of forest and mine roads has significantly intensified the rates of forest fragmentation and degradation in the OCAs of the roads since the 1980s. To mitigate these high amounts of forest changes, the integration of the unprotected forests to the protected areas and the prevention of destructive operations such as the open-cast mining and coincident logging and mining in the Hyrcanian forests are inevitable. Clearly, further research is necessary to demonstrate the negative impacts of the dimensions of these forest changes on the biodiversity, forest functionalities, natural hazards, water resources, and indigenous inhabitants of the Hyrcanian forests.

ACKNOWLEDGMENTS

This study is a part of the first author's doctoral dissertation under the supervision of the third author. The authors would like to thank anonymous reviewers and the editors for their constructive comments and suggestions, which greatly improved the quality of the manuscript.

ORCID

Zeinab Shirvani https://orcid.org/0000-0002-2882-850X
Omid Abdi https://orcid.org/0000-0002-8048-8792
Manfred F. Buchroithner https://orcid.org/0000-0002-6051-2249

ENDNOTE

[1] A channel is defined as a slice of wavelengths in the spectrum of electromagnetic such as blue, green, and red (Adams & Gillespie, 2006).

REFERENCES

Abdi, O., Kamkar, B., Shirvani, Z., Teixeira da Silva, J. A., & Buchroithner, M. F. (2018). Spatial-statistical analysis of factors determining forest fires: A case study from Golestan, northeast Iran. *Geomatics, Natural Hazards and Risk*, *9*(1), 267–280. https://doi.org/10.1080/19475705.2016.1206629

Abdi, O., Shirvani, Z., & Buchroithner, M. F. (2018). Visualization and quantification of significant anthropogenic drivers influencing rangeland degradation trends using Landsat imagery and GIS spatial dependence models: A case study in Northeast Iran. *Geographical Sciences*, *28*(12), 1933–1952. https://doi.org/10.1007/s11442-018-1572-z

Adams, J. B., & Gillespie, A. R. (2006). *Remote sensing of landscapes with spectral images: A physical modeling approach*. Cambridge University Press, Cambridge, UK. ISBN 0-521-66221-4.

Aguilar, F., Nemmaoui, A., Aguilar, M., Chourak, M., Zarhloule, Y., & García Lorca, A. (2016). A quantitative assessment of forest cover change in the Moulouya River watershed (Morocco) by the integration of a subpixel-based and object-based analysis of Landsat data. *Forests*, *7*(1), 23. https://doi.org/10.3390/f7010023

Akhani, H., & Ziegler, H. (2002). Photosynthetic pathways and habitats of grasses in Golestan National Park (NE Iran), with an emphasis on the C4-grass dominated rock communities. *Phytocoenologia*, *32*, 455–501. https://doi.org/10.1127/0340-269X/2002/0032-0455

Alamgir, M., Campbell, M. J., Sloan, S., Goosem, M., Clements, G. R., Mahmoud, M. I., & Laurance, W. F. (2017). Economic, socio-political and environmental risks of road development in the tropics. *Current Biology*, *27*(20), R1130–R1140. https://doi.org/10.1016/j.cub.2017.08.067

Ali, J., Benjaminsen, T. A., Hammad, A. A., & Dick, Ø. B. (2005). The road to deforestation: An assessment of forest loss and its causes in Basho Valley, northern Pakistan. *Global Environmental Change*, *15*(4), 370–380. https://doi.org/10.1016/j.gloenvcha.2005.06.004

Alvarez-Berríos, N. L., & Aide, T. M. (2015). Global demand for gold is another threat for tropical forests. *Environmental Research Letters*, *10*(1), 014006. https://doi.org/10.1088/1748-9326/10/1/014006

Anderson JR. 1976. A land use and land cover classification system for use with remote sensor data (Vol. 964): United States Government Printing Office, Washington. https://doi.org/10.3133/pp964

Anselin, L. (1995). Local indicators of spatial association—LISA. *Geographical Analysis*, *27*(2), 93–115. https://doi.org/10.1111/j.1538-4632.1995.tb00338.x

Anselin, L., & Rey, S. J. (2014). *Modern spatial econometrics in practice: A guide to GeoDa*. GeoDaSpace and PySAL: GeoDa Press.

Anselin, L., Syabri, I., & Kho, Y. (2006). GeoDa: An introduction to spatial data analysis. *Geographical Analysis*, *38*(1), 5–22. https://doi.org/10.1111/j.0016-7363.2005.00671.x

Anselin, L., Syabri, I., & Smirnov, O. (2002). Visualizing multivariate spatial correlation with dynamically linked windows. In *Proceedings: CSISS workshop on new tools for spatial data analysis. May* (p. 2002). Santa Barbara: CA.

Arima, E. Y., Walker, R. T., Perz, S. G., & Caldas, M. (2005). Loggers and forest fragmentation: Behavioral models of road building in the Amazon Basin. *Annals of the Association of American Geographers*, *95*(3), 525–541. https://doi.org/10.1111/j.1467-8306.2005.00473.x

Asner, G. P., Llactayo, W., Tupayachi, R., & Luna, E. R. (2013). Elevated rates of gold mining in the Amazon revealed through high-resolution monitoring. *Proceedings of the National Academy of Sciences*, *110*(46), 18454–18459. https://doi.org/10.1073/pnas.1318271110

Badraghi, N., Erler, J., & Hosseini, S. A. O. (2015). Residual damage in different ground logging methods alongside skid trails and winching strips. *Journal of Forest Science*, *61*(12), 526–534. https://doi.org/10.17221/50/2015-JFS

Barber, C. P., Cochrane, M. A., Souza, C. M., & Laurance, W. F. (2014). Roads, deforestation, and the mitigating effect of protected areas in the Amazon. *Biological Conservation*, *177*, 203–209. https://doi.org/10.1016/j.biocon.2014.07.004

Bebbington, A. J., Bebbington, D. H., Sauls, L. A., Rogan, J., Agrawal, S., Gamboa, C., … Royo, A. (2018). Resource extraction and infrastructure threaten forest cover and community rights. *Proceedings of the National Academy of Sciences*, *115*(52), 13164–13173. https://doi.org/10.1073/pnas.1812505115.

Belgiu, M., Drăguţ{t\hskip-0.7ex\char "B8}, L., & Strobl, J. (2014). Quantitative evaluation of variations in rule-based classifications of land cover in urban neighbourhoods using WorldView-2 imagery. *ISPRS Journal of Photogrammetry and Remote Sensing*, *87*, 205–215. https://doi.org/10.1016/j.isprsjprs.2013.11.007

Bell, F. G., & Donnelly, L. J. (2014). *Mining and its impact on the environment*. London: CRC Press.

Boston, K. (2016). The potential effects of forest roads on the environment and mitigating their impacts. *Current Forestry Reports*, *2*(4), 215–222. https://doi.org/10.1007/s40725-016-0044-x

Bruijnzeel, L. A. (2004). Hydrological functions of tropical forests: Not seeing the soil for the trees? *Agriculture, Ecosystems & Environment*, *104*(1), 185–228. https://doi.org/10.1016/j.agee.2004.01.015

Buckley, D. S., Crow, T. R., Nauertz, E. A., & Schulz, K. E. (2003). Influence of skid trails and haul roads on understory plant richness and composition in managed forest landscapes in upper Michigan, USA. *Forest Ecology and Management*, *175*(1), 509–520. https://doi.org/10.1016/s0378-1127(02)00185-8

Butsic, V., Baumann, M., Shortland, A., Walker, S., & Kuemmerle, T. (2015). Conservation and conflict in the Democratic Republic of Congo: The impacts of warfare, mining, and protected areas on deforestation. *Biological Conservation*, *191*, 266–273. https://doi.org/10.1016/j.biocon.2015.06.037

Butt, N., Beyer, H. L., Bennett, J. R., Biggs, D., Maggini, R., Mills, M., … Possingham, H. P. (2013). Biodiversity risks from fossil fuel extraction. *Science*, *342*(6157), 425–426. https://doi.org/10.1126/science.1237261

Caballero Espejo, J., Messinger, M., Román-Dañobeytia, F., Ascorra, C., Fernandez, L., & Silman, M. (2018). Deforestation and forest degradation due to gold mining in the Peruvian Amazon: A 34-year perspective. *Remote Sensing*, *10*(12), 1903. https://doi.org/10.3390/rs10121903

Caspian Hyrcanian Forest Project (CHFP). (2013). *Building a multiple use forest management framework to conserve biodiversity in the Caspian forest landscape* (p. 203. (In Persian)). Iran: Document of UNDP/GEF/FRWO Caspian Hyrcanian Forest Project. http://chfp.ir/index.php/aabout/category/1-2016-07-18-09-59-25 [accessed October 31, 2019].

Chavez, P. S. (1988). An improved dark-object subtraction technique for atmospheric scattering correction of multispectral data. *Remote*

Sensing of Environment, *24*(3), 459–479. https://doi.org/10.1016/0034-4257(88)90019-3

Chomitz, K. M., & Gray, D. A. (1996). Roads, land use, and deforestation: A spatial model applied to Belize. *World Bank Economic Review*, *10*(3), 487–512. https://doi.org/10.1093/wber/10.3.487

Clements, G. R., Lynam, A. J., Gaveau, D., Yap, W. L., Lhota, S., & Goosem, M. (2014). Where and how are roads endangering mammals in Southeast Asia's forests? *PLoS One*, *9*(12), e115376. https://doi.org/10.1371/journal.pone.0115376

Cliff, A. D., & Ord, J. K. (1973). *Spatial autocorrelation*. London: Pion. ISBN-10: 0850860377.

Cudzik, A., Brennensthul, M., Białczyk, W., & Czarnecki, J. (2017). Damage to soil and residual trees caused by different logging systems applied to late thinning. *Croatian Journal of Forest Engineering: Journal for Theory and Application of Forestry Engineering*, *38*(1), 83–95.

Desclée, B., Bogaert, P., & Defourny, P. (2006). Forest change detection by statistical object-based method. *Remote Sensing of Environment*, *102*(1–2), 1–11. https://doi.org/10.1016/j.rse.2006.01.013

Dorren, L. K. A., Maier, B., & Seijmonsbergen, A. C. (2003). Improved Landsat-based forest mapping in steep mountainous terrain using object-based classification. *Forest Ecology and Management*, *183*(1), 31–46. https://doi.org/10.1016/S0378-1127(03)00113-0

Douglas, I. (2003). Predicting road erosion rates in selectively logged tropical rain forests. In D. H. de Boer, W. Froehlich, T. Mizuyana, & A. Pietroniro (Eds.), *Erosion prediction in ungauged basins: Integrating methods and techniques* (Vol. 279, pp. 199–205). Wallingford, UK: IAHS Press.

Douglas, R. A. (2017). *Low-volume road engineering: Design, construction, and maintenance*. Boca Raton: Taylor & Francis Group. ISBN 9781138748156

Eitzel, M., Kelly, M., Dronova, I., Valachovic, Y., Quinn-Davidson, L., Solera, J., & de Valpine, P. (2016). Challenges and opportunities in synthesizing historical geospatial data using statistical models. *Ecological Informatics*, *31*, 100–111. https://doi.org/10.1016/j.ecoinf.2015.11.011

Ernst, C., Verhegghen, A., Bodart, C., Mayaux, P., de Wasseige, C., Bararwandika, A., et al. (2010). Congo Basin forest cover change estimate for 1990, 2000 and 2005 by Landsat interpretation using an automated object-based processing chain. *International Archives of the Photogrammetry, Remote Sensing and Spatial Information Sciences*, *XXXVIII-4/C7*, 1–6.

Fan, C., & Myint, S. (2014). A comparison of spatial autocorrelation indices and landscape metrics in measuring urban landscape fragmentation. *Landscape and Urban Planning*, *121*, 117–128. https://doi.org/10.1016/j.landurbplan.2013.10.002

Fischer, J., & Lindenmayer, D. B. (2007). Landscape modification and habitat fragmentation: A synthesis. *Global Ecology and Biogeography*, *16*(3), 265–280. https://doi.org/10.1111/j.1466-8238.2007.00287.x

Gómez, D., Biging, G., & Montero, J. (2008). Accuracy statistics for judging soft classification. *International Journal of Remote Sensing*, *29*, 693–709. https://doi.org/10.1080/01431160701311325

Gullison, R. E., & Hardner, J. J. (1993). The effects of road design and harvest intensity on forest damage caused by selective logging: Empirical results and a simulation model from the Bosque Chimanes, Bolivia. *Forest Ecology and Management*, *59*, 1), 1–1), 14. https://doi.org/10.1016/0378-1127(93)90067-W

Hald, A. (1952). *Statistical theory with engineering applications* Statistical theory with engineering applications. New York: John Wiley & Sons.

Halounová, L. (2003). Textural classification of B&W aerial photos for the forest classification. In: *Proceedings of 23rd symposium of European association of remote sensing laboratories (EARSEL), Gent, Belgium*, 173–179.

Hawbaker, T. J., Radeloff, V. C., Clayton, M. K., Hammer, R. B., & Gonzalez-Abraham, C. E. (2006). Road development, housing growth, and landscape fragmentation in northern Wisconsin: 1937–1999. *Ecological Applications*, *16*(3), 1222–1237. https://doi.org/10.1890/1051-0761(2006)016[1222:RDHGAL]2.0.CO;2

Heilman, G. E., Strittholt, J. R., Slosser, N. C., & Dellasala, D. A. (2002). Forest fragmentation of the conterminous United States: Assessing forest intactness through road density and spatial characteristics forest fragmentation can be measured and monitored in a powerful new way by combining remote sensing, geographic information systems. *And Analytical Software. BioScience*, *52*(5), 411–422. https://doi.org/10.1641/0006-3568(2002)052[0411:FFOTCU]2.0.CO;2

Hermosilla, T., Wulder, M. A., White, J. C., Coops, N. C., & Hobart, G. W. (2015). Regional detection, characterization, and attribution of annual forest change from 1984 to 2012 using Landsat-derived time-series metrics. *Remote Sensing of Environment*, *170*, 121–132. https://doi.org/10.1016/j.rse.2015.09.004

Islamic Consultative Assembly of Iran (ICA). (2003). Comprehensive plan for conservation the northern forests of the country (conservation, maintenance and development of the northern forests). Retrieved from http://www.hvm.ir/lawdetailnews.aspx?id=34883.

Jamshidi, R., Jaeger, D., Raafatnia, N., & Tabari, M. (2008). Influence of two ground-based skidding systems on soil compaction under different slope and gradient conditions. *International Journal of Engineering Science*, *19*(1), 9–16. https://doi.org/10.1080/14942119.2008.10702554

Japan International Cooperation Agency (JICA), 2006. Flood and debris flow in the Caspian coastal and focusing on the flood-hit region in Golestan Province. Final report, Volume III-1 supporting report I: master plan. Ministry of Jihad-e-agriculture, the Islamic Republic of Iran, October 2006, Golestan, Iran. 54 pages.

Jiang, Z., Huete, A. R., Didan, K., & Miura, T. (2008). Development of a two-band enhanced vegetation index without a blue band. *Remote Sensing of Environment*, *112*(10), 3833–3845. https://doi.org/10.1016/j.rse.2008.06.006

Jourgholami, M. (2012). Operational impacts to residual stands following ground-based skidding in Hyrcanian forest, northern Iran. *Journal of Forestry Research*, *23*(2), 333–333, 337. https://doi.org/10.1007/s11676-012-0261-5

Jourgholami, M., & Majnounian, B. (2011). Harvesting systems in Hyrcanian forest, Iran; limitations and approaches. The forest engineering network (Formec, Austria, Proceedings) October 2011: 9–13.

Jusys, T. (2016). Fundamental causes and spatial heterogeneity of deforestation in legal Amazon. *Applied Geography*, *75*, 188–199. https://doi.org/10.1016/j.apgeog.2016.08.015

Keller, G., & Sherar, J. (2003). Low-volume roads engineering: Best management practices. *Transportation Research Record: Journal of the Transportation Research Board*, *1819*, 174–181. https://doi.org/10.3141/1819a-25

Kennedy, R. E., Andréfouët, S., Cohen, W. B., Gómez, C., Griffiths, P., Hais, M., … Zhu, Z. (2014). Bringing an ecological view of change to Landsat-based remote sensing. *Frontiers in Ecology and the Environment*, *12*(6), 339–346. https://doi.org/10.1890/130066

Kleinschroth, F., Gourlet-Fleury, S., Gond, V., Sist, P., & Healey, J. R. (2016). Logging roads in tropical forests: Synthesis of literature written in French and English highlights environmental impact reduction through improved engineering. *Bois et Forêts Des Tropiques, N*, *328*(2), 13–26. https://doi.org/10.19182/bft2016.328.a31299

Knapp, H. D. (2005). Die globale Bedeutung der Kaspischen Wälder. In Nosrati, K., Marvie Mohadjer, R., Bode, W. and Knapp, H. D., Schutz der Biologischen Vielfalt und integriertes Management der Kaspischen Wälder (Nordiran). Bundesamt für Naturschutz, 45–70.

La Marche, J. L., & Lettenmaier, D. P. (2001). Effects of forest roads on flood flows in the Deschutes River, Washington. *Earth Surface Processes and Landforms*, *26*(2), 115–134. https://doi.org/10.1002/1096-9837(200102)26:2<115::AID-ESP166>3.0.CO;2-O

Laurance, W. F. (2000). Do edge effects occur over large spatial scales? *Trends in Ecology & Evolution*, *15*(4), 134–135. https://doi.org/10.1016/S0169-5347(00)01838-3

Laurance, W. F., Cochrane, M. A., Bergen, S., Fearnside, P. M., Delamônica, P., Barber, C., … Fernandes, T. (2001). The future of the Brazilian Amazon. *Science*, *291*(5503), 438–439. https://doi.org/10.1126/science.291.5503.438

Laurance, W. F., Goosem, M., & Laurance, S. G. W. (2009). Impacts of roads and linear clearings on tropical forests. *Trends in Ecology & Evolution*, *24*(12), 659–669. https://doi.org/10.1016/j.tree.2009.06.009

Laurance, W. F., Lovejoy, T. E., Vasconcelos, H. L., Bruna, E. M., Didham, R. K., Stouffer, P. C., … Sampaio, E. (2002). Ecosystem decay of Amazonian Forest fragments: A 22-year investigation. *Conservation Biology*, *16*(3), 605–618. https://doi.org/10.1046/j.1523-1739.2002.01025.x

Lees, A. C., & Peres, C. A. (2009). Gap-crossing movements predict species occupancy in Amazonian forest fragments. *Oikos*, *118*(2), 280–290. https://doi.org/10.1111/j.1600-0706.2008.16842.x

Lewinski, S., Bochenek, Z., & Turlej, K. (2010). Application of object-oriented method for classification of VHR satellite images using rule-based approach and texture measures. *Geoinformation Issues*, *2*(1), 19–26.

MacDonagh, P., Rivero, L., Garibaldi, J., Alvez, M., Cortez, P., Marek, M., … Toma, T. (2010). Effects of selective harvesting on traffic pattern and soil compaction in a subtropical forest in Guarani, Misiones, Argentine. *Scientia Forestalis/Forest Sciences*, *38*(85), 343–352.

Malmer, A., & Grip, H. (1990). Soil disturbance and loss of infiltrability caused by mechanized and manual extraction of tropical rainforest in Sabah, Malaysia. *Forest Ecology and Management*, *38*(1-2), 1–12. https://doi.org/10.1016/0378-1127(90)90081-L

McGarigal, K., & Marks, B. J. (1995). *FRAGSTATS: Spatial pattern analysis program for quantifying landscape structure*. *General Technical Report*. PNW-GTR-351. Portland, OR: U.S. Department of Agriculture, Forest Service, Pacific Northwest Research Station. 122 p. http://www.umass.edu/landeco/research/fragstats/fragstats.html

McIntyre, S., & Hobbs, R. (1999). A framework for conceptualizing human effects on landscapes and its relevance to management and research models. *Conservation Biology*, *13*(6), 1282–1292. https://doi.org/10.1046/j.1523-1739.1999.97509

Mena, C. F., Laso, F., Martinez, P., & Sampedro, C. (2017). Modeling road building, deforestation and carbon emissions due deforestation in the Ecuadorian Amazon: The potential impact of oil frontier growth. *Journal of Land Use Science*, *12*(6), 477–492. https://doi.org/10.1080/1747423X.2017.1404648

Miranda, M., Burris, P., Bingcang, J. F., Shearman, P., Briones, J. O., La Viña, A., … Mooney, C. (2003). *Mining and critical ecosystems: mapping the risks*. World Resources Institute, Washington DC, *58*.

Modrý, M., & Hubený, D. (2003). Impact of skidder and high-lead system logging on forest soils and advanced regeneration. *Journal of Forest Science*, *49*(6), 273–280. https://doi.org/10.17221/4701-JFS

Narayanaraj, G., & Wimberly, M. C. (2012). Influences of forest roads on the spatial patterns of human- and lightning-caused wildfire ignitions. *Applied Geography*, *32*(2), 878–888. https://doi.org/10.1016/j.apgeog.2011.09.004

Navulur, K. (2006). *Multispectral image analysis using the object-oriented paradigm*. Boca Raton: CRC Press.

Newman, M. E., McLaren, K. P., & Wilson, B. S. (2014). Assessing deforestation and fragmentation in a tropical moist forest over 68 years; the impact of roads and legal protection in the cockpit country, Jamaica. *Forest Ecology and Management*, *315*, 138–152. https://doi.org/10.1016/j.foreco.2013.12.033

Potapov, P., Hansen, M. C., Laestadius, L., Turubanova, S., Yaroshenko, A., Thies, C., … Esipova, E. (2017). The last frontiers of wilderness: Tracking loss of intact forest landscapes from 2000 to 2013. *Science Advances*, *3*(1), e1600821. https://doi.org/10.1126/sciadv.1600821

Raši, R., Beuchle, R., Bodart, C., Vollmar, M., Seliger, R., & Achard, F. (2013). Automatic updating of an object-based tropical forest cover classification and change assessment. *IEEE Journal of Selected Topics in Applied Earth Observations and Remote Sensing*, *6*(1), 66–73. https://doi.org/10.1109/JSTARS.2012.2217733

Rezaee, S. K., & Moayeri, M. H. (2014). Assessment of enforcing the arrangement plan of forest dwellers and out of livestock from forests. *Journal of Forest and Range*, *101*, 6–14 (in Persian). http://frw.org.ir/00/Fa/StaticPages/Page.aspx?tid=1509

Riitters, K., Wickham, J., Neill, R., Jones, B., & Smith, E. (2000). Global-scale patterns of forest fragmentation. *Conservation Ecology*, *4*(2). [online] URL: http://www.consecol.org/vol4/iss2/art3

Sagheb-Talebi, K., Sajedi, T., Pourhashemi, M. (2014). Forests of Iran: A treasure from the past, a hope for the future. In Plant and Vegetation, M. J. A Werger (ed.), (Vol. 10): Springer Science & Business Media: Dordrecht. https://doi.org/10.1007/978-94-007-7371-4

Sessions, J. (2007). *Forest road operations in the tropics*. Berlin/Heidelberg: Springer, 170. https://doi.org/10.1007/978-3-540-46393-1

Shirvani, Z., Abdi, O., Buchroithner, M. F., & Pradhan, B. (2017). Analysing spatial and statistical dependencies of deforestation affected by residential growth: Gorganrood Basin, Northeast Iran. *Land Degradation & Development*, *28*(7), 2176–2190. https://doi.org/10.1002/ldr.2744

Sidle, R. C., Sasaki, S., Otsuki, M., Noguchi, S., & Rahim Nik, A. (2004). Sediment pathways in a tropical forest: Effects of logging roads and skid trails. *Hydrological Processes*, *18*(4), 703–720. https://doi.org/10.1002/hyp.1364

Sonter, L. J., Herrera, D., Barrett, D. J., Galford, G. L., Moran, C. J., & Soares-Filho, B. S. (2017). Mining drives extensive deforestation in the Brazilian Amazon. *Nature Communications*, *8*, 1013. https://doi.org/10.1038/s41467-017-00557-w

Southworth, J., Munroe, D., & Nagendra, H. (2004). Land cover change and landscape fragmentation—Comparing the utility of continuous and discrete analyses for a western Honduras region. *Agriculture, Ecosystems & Environment*, *101*(2), 185–205. https://doi.org/10.1016/j.agee.2003.09.011

Statistical Center of Iran (SCI). (1966). *The population and housing censuses* (In Persian). Retrieved from Tehran: http://www.amar.org.ir [accessed on 24 October–November 13, 2011].

Statistical Center of Iran (SCI). (1986). *The population and housing censuses* (In Persian). Retrieved from Tehran: http://www.amar.org.ir [accessed on 24 October–November 13, 2011].

Statistical Center of Iran (SCI). (1996). *The population and housing censuses* (In Persian). Retrieved from Tehran: http://www.amar.org.ir [accessed on 24 October–November 13, 2011].

Statistical Center of Iran (SCI). (2011). *The population and housing censuses* (In Persian). Retrieved from Tehran: http://www.amar.org.ir *[accessed on September 15, 2015]*.

Statistical Center of Iran (SCI). (2016). *The population and housing censuses* (In Persian). Retrieved from Tehran: http://www.amar.org.ir [accessed on April 2017].

Tannant, D., & Regensburg, B. (2001). *Guidelines for mine haul road design*. The University of British Columbia. https://doi.org/10.14288/1.0102562

Teillet, P. M., Guindon, B., & Goodenough, D. G. (1982). On the slope-aspect correction of multispectral scanner data. *Canadian Journal of Remote Sensing*, *8*(2), 84–106. https://doi.org/10.1080/07038992.1982.10855028

Tejaswi, G. (2007). *Manual on deforestation, degradation, and fragmentation using remote sensing and GIS: Strengthening monitoring, assessment and reporting (MAR) on sustainable Forest management (SFM) in Asia (GCP/INT/988/JPN): MAR-SFM working paper 5/2007*. *Forestry department*. Rome: FAO.

Trombulak, S. C., & Frissell, C. A. (2000). Review of ecological effects of roads on terrestrial and aquatic communities. *Conservation Biology*, *14*(1), 18–30. https://doi.org/10.1046/j.1523-1739.2000.99084.x

Tsioras, P. A., & Liamas, D. K. (2015). Residual tree damage along skidding trails in beech stands in Greece. *Forest Research*, *26*(2), 523–531. https://doi.org/10.1007/s11676-015-0056-6

Uddin, K., Chaudhary, S., Chettri, N., Kotru, R., Murthy, M., Chaudhary, R. P., … Gautam, S. K. (2015). The changing land cover and fragmenting forest on the roof of the world: A case study in Nepal's Kailash sacred landscape. *Landscape and Urban Planning*, *141*, 1–10. https://doi.org/10.1016/j.landurbplan.2015.04.003

Van Der Hoeven, C. A., De Boer, W. F., & Prins, H. H. (2010). Roadside conditions as predictor for wildlife crossing probability in a central African rainforest. *African Journal of Ecology*, *48*(2), 368–377. https://doi.org/10.1111/j.1365-2028.2009.01122.x

Willhauck, G., Schneider, T., De Kok, R., & Ammer, U. (2000). Comparison of object oriented classification techniques and standard image analysis for the use of change detection between SPOT multispectral satellite images and aerial photos. Paper presented at the Proceedings of XIX ISPRS Congress.

Young, N. E., Anderson, R. S., Chignell, S. M., Vorster, A. G., Lawrence, R., & Evangelista, P. H. (2017). A survival guide to Landsat preprocessing. *Ecology*, *98*(4), 920–932. https://doi.org/10.1002/ecy.1730

Ziaei, Z., Pradhan, B., & Mansor, S. B. (2014). A rule-based parameter aided with object-based classification approach for extraction of building and roads from WorldView-2 images. *Geocarto International*, *29*(5), 554–569. https://doi.org/10.1080/10106049.2013.819039

How to cite this article: Shirvani Z, Abdi O, Buchroithner MF. A new analysis approach for long-term variations of forest loss, fragmentation, and degradation resulting from road-network expansion using Landsat time-series and object-based image analysis. *Land Degrad Dev*. 2020;31:1462–1481. https://doi.org/10.1002/ldr.3530